AGU PUBLICATIONS

Tectonics

RESEARCH ARTICLE
10.1002/2012TC003221

Key Points:
- Fast rock uplift and basin subsidence during late Paleocene-early Eocene
- Uplift became younger southwestward during late Paleocene-early Eocene
- Laramide deformation was caused by flat slab subduction and slab removal

Correspondence to:
M. Fan,
mfan@uta.edu

Citation:
Fan, M., and B. Carrapa (2014), Late Cretaceous–early Eocene Laramide uplift, exhumation, and basin subsidence in Wyoming: Crustal responses to flat slab subduction, *Tectonics*, *33*, doi:10.1002/2012TC003221.

Received 24 AUG 2012
Accepted 5 MAR 2014
Accepted article online 13 MAR 2014

Late Cretaceous–early Eocene Laramide uplift, exhumation, and basin subsidence in Wyoming: Crustal responses to flat slab subduction

Majie Fan[1] and Barbara Carrapa[2]

[1]Department of Earth and Environmental Sciences, University of Texas at Arlington, Arlington, Texas, USA, [2]Department of Geosciences, University of Arizona, Tucson, Arizona, USA

Abstract Low-angle subduction of the Farallon oceanic plate during the Late Cretaceous–early Eocene is generally considered as the main driver forming the high Rocky Mountains in Wyoming and nearby areas. How the deformation was transferred from mantle to upper crust over the great duration of deformation (~40 Myr) is still debated. Here, we reconstruct basin subsidence and compile paleoelevation, thermochronology, and provenance data to assess the timing, magnitude, and rates of rock uplift during the Laramide deformation. We reconstruct rock uplift as the sum of surface uplift and erosion constrained by combining paleoelevation and exhumation with regional stratigraphic thickness and chronostratigraphic information. The amount (and rate) of rock uplift of individual Laramide ranges was less than 2.4–4.8 km (~0.21–0.32 mm/yr) during the early Maastrichtian-Paleocene (stage 1) and increased to more than ~3 km (~0.38–0.60 mm/yr) during the late Paleocene–early Eocene (stage 2). Our quantitative constraints reveal a two-stage development of the Laramide deformation in Wyoming and an increase of rock uplift during stage 2, associated with enhanced intermontane basin subsidence. Exhumation and uplift during stage 1 is consistent with eastward migration of Cordilleran deformation associated with low-angle subduction, whereas the change in exhumation during stage 2 seems to follow a southwestward trend, which requires an alternative explanation. We here suggest that the increase of rock uplift rate during the late Paleocene–early Eocene and the southwestward younging trend of uplift may be a response to the rollback and associated retreating delamination of the Farallon oceanic slab.

1. Introduction

The Rocky Mountains in southern Montana, Wyoming, and northern Colorado are an extensive area of high relief forming the eastern part of the North American Cordillera (Figure 1). The average elevation of the mountains ranges in the region is 2–3 km with peaks >4 km, whereas the intermontane basin floors are ~ 1.5 km high. Beginning during Late Jurassic time, the region was the site of the Cordilleran foreland basin associated with thin-skinned deformation and flexural loading of the Cordilleran fold-and-thrust belt. Regional flexural subsidence continued until ~81 Ma based on evidence provided by the occurrence of thick Cretaceous marine and marginal-marine deposits and basin geometry [e.g., *Jordan*, 1981; *Cross*, 1989; *Roberts and Kirschbaum*, 1995; *DeCelles*, 2004; *Painter and Carrapa*, 2013]. Subsequent thick-skinned deformation (Laramide orogeny) partitioned the regional foreland basin and caused more than 4 km of localized exhumation of crystalline basement blocks, accompanied by localized subsidence of intermontane basins until ~45 Ma [e.g., *Dickinson and Snyder*, 1978; *Dickinson et al.*, 1988; *DeCelles*, 2004; *Cather et al.*, 2012]. It is generally accepted that the switch of deformation style from thin-skinned to thick-skinned was caused by the change from normal high-angle subduction to low-angle subduction of buoyant Farallon oceanic lithosphere beneath western North America [e.g., *Snyder et al.*, 1976; *Coney and Reynolds*, 1977; *Livaccari et al.*, 1981; *Henderson et al.*, 1984; *Erslev*, 1993; *Bird*, 1998; *Tarduno et al.*, 1985; *Saleeby*, 2003; *DeCelles*, 2004; *Liu et al.*, 2008; *Humphreys*, 2009; *L. Liu et al.*, 2010; *Z. Liu et al.*, 2010; *Jones et al.*, 2011]. The thin Paleozoic-Mesozoic sedimentary sequence in Wyoming and its nearby area may have promoted the development of thick-skinned structures [*DeCelles*, 2004]. However, the exhumational response of individual basement-cored mountains to low-angle subduction is not well understood, nor is it clear how the duration (~40 Myr) of the Laramide orogeny reconciles with the eastward propagation of the Cordilleran deformation front [e.g., *Erslev*, 1993; *DeCelles*, 2004; *Jones et al.*, 2011].

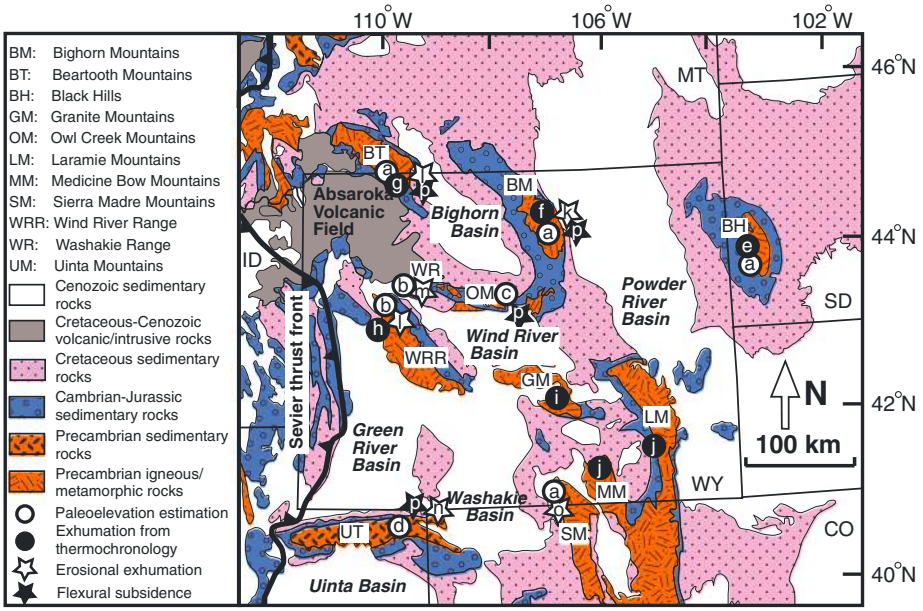

Figure 1. Simplified geological map of the Rocky Mountains in Wyoming showing studied sites of each set of data. Paleoaltimetry: (a) *Dettman and Lohmann* [2000] and *Fan and Dettman* [2009]; (b) *Fan et al.* [2011a]; (c) *Chamberlain et al.* [2012]; (d) *Norris et al.* [1996], *Davis et al.* [2008], and *Wolfe et al.*, [1998]. Thermochronology: (e) *Strecker* [1996], (f) *Crowley et al.* [2002] and *Peyton et al.* [2012]; (g) *Omar et al.* [1994], *Crowley et al.* [2002], and *Peyton et al.* [2012]; (h) *Cerveny and Steidtmann* [1993], *Peyton et al.* [2012], and this study; (i) *LeFebre* [1988]; (j) *Cerveny* [1990], *Kelley* [2005], and *Peyton et al.* [2012]. Erosional exhumation: (k) *Hoy and Ridgway*, 1997 and *Fan et al.* [2011b]; (l) *DeCelles et al.* [1991]; (m) *Winterfeld and Conard* [1983], *Steidtmann and Middleton* [1991], *Fan et al.* [2011a, 2011b]; (n) *Crews and Ethridge* [1993] and *Fan et al.* [2011b]; (o) *Fan et al.* [2011b]. Basin subsidence: (p) this study.

Many geodynamic models have been proposed to explain the tectonic processes that have uplifted the Rocky Mountains. Such models make different predictions about the pattern, magnitude, and rate of Laramide deformation. These models can be broadly grouped into two categories based on the deformation mechanisms. First, low-angle subduction of a segment of the Farallon plate (perhaps an aseismic ridge or oceanic plateau) induced uplift through basal traction on the North American plate [e.g., *Bird*, 1988; *Saleeby*, 2003], lateral movement of lower crustal material [*McQuarrie and Chase*, 2000], adding end load at the trench, possibly with the strong Colorado Plateau as an opposing end load [e.g., *Livaccari*, 1991; *Jones et al.*, 1998], and increased deviatoric horizontal stresses by the downward displacement of the lithosphere above the asthenosphere wedge [*Jones et al.*, 2011]. This set of models predicts that surface and rock uplift of the Laramide basement-cored mountains and subsidence of the intermontane basins should follow the overall northeastward subduction direction. Alternatively, removal of ecologitized oceanic plateaux induced dynamic uplift through upwelling of hot mantle [*Liu et al.*, 2008; *Humphreys*, 2009; *L. Liu et al.*, 2010; *Liu and Gurnis*, 2010]. This second group of models predicts that Laramide deformation may be divided into two stages in response to the northeastward low-angle subduction and subsequent removal of the plateaux [*Liu and Gurnis*, 2010].

Several geodynamic modeling studies have shown that slab rollback or steepening can directly cause surface deformation and uplift through isostatic, dynamic, and thermal processes [e.g., *Gvirtzman and Amos*, 1999; *Buiter et al.*, 2002; *Göğüş et al.*, 2011]. Slab rollback can additionally induce surface deformation by delaminating the mantle lithosphere of the overriding continental plate [*Brun and Faccenna*, 2008; *Göğüş et al.*, 2011]. Although slab rollback is often associated with extensional tectonics in the overriding plate, *Ferranti and Oldow* [2006] documented synchronous foreland uplift and hinterland extension in the southern Appennines orogen associated with the rollback of the subducted Adriatic slab. In the southern Puna Plateau-Sierras Pampeanas in South America, an analogue of the Sevier-Laramide province in the Cordilleran orogenic belt, rollback of the low-angle subducted Nazca oceanic plate, and induced mantle lithosphere delamination of the overriding continental plate have been suggested as driving the uplift of

the thick-skinned Sierras Pampeanas [*Kay and Coira*, 2009]. Although rollback of the subducting Farallon oceanic slab has not been invoked as a geodyamic model to explain the Laramide deformation, slab rollback from ~55 Ma to 48 Ma underneath Wyoming has been inferred from the westward migration of arc magmatism [*Constenius*, 1996]. This westward migration of magmatism is younger than the migration in the southern Rocky Mountains [*Coney and Reynolds*, 1977]. Slab rollback during the early Eocene is also inferred to have produced low-angle detachment faults, metamorphic core complexes, and half graben basins representing extensional tectonic setting in the Sevier hinterland as early as ~54 Ma [e.g., *Constenius*, 1996; *Foster et al*., 2007; *Cubley et al*., 2013]. Although eclogitization of a subducted oceanic plateau has been invoked to explain the Laramide deformation [*Liu et al*., 2008; *L. Liu et al*., 2010], the role that slab rollback played in the surface deformation during the Laramide orogeny remains unclear.

Evaluation of the different geodynamic models requires analysis of the timing, rates, and patterns of rock uplift [*sensu England and Molnar*, 1990] over the long duration of Laramide deformation during the Late Cretaceous–early Eocene. In this paper, we reconstruct the subsidence history of the major Laramide intermontane basins (Powder River, Bighorn, Wind River, and Green River basins) in Wyoming and compile paleoaltimetry, sedimentology, geochemistry, geochronology, and thermochronology data sets in order to resolve the timing and magnitude of surface and rock uplift of the Laramide mountain ranges. The resulting synthesis shows that the Laramide deformation had two stages of development in Wyoming and nearby areas, consistent with the previous observation made from regional structures and sedimentation [*Chapin and Cather*, 1983; *Gries*, 1983; *Chapin and Cather*, 1990]. Our study shows increased surface elevation gain and rate of rock uplift in the Laramide mountain ranges during the late Paleocene–early Eocene, accompanied by increased subsidence rates in the major Laramide intermontane basins and a southwestward younging of exhumation. Whereas the Maastrichtian to Paleocene history can be explained by flat-slab subduction, we interpret the acceleration during the late Paleocene–early Eocene to be the result of slab rollback.

2. Laramide Intermontane Basin Subsidence

2.1. Isopach of Basin Fill

Basin subsidence history can be reconstructed using isopachs of sedimentary basin fill. Flexure of the lithosphere in response to topographic loading produces elongated accommodation space near the load [e.g., *Beaumont*, 1981; *Jordan*, 1981]. The sediment accommodation space diminishes away from the load, resulting in a distinct foredeep geometry adjacent to the mountain front [e.g., *Jordan*, 1981; *DeCelles and Giles*, 1996]. Major Laramide intermontane basins in Wyoming are asymmetric in cross section, with fills that thicken toward the adjacent reverse-fault-bounded uplifts [e.g., *Keefer*, 1965; *Royse et al*., 1975], representing flexural subsidence induced by topographic loading of the Laramide mountain ranges [*Hagen et al*., 1985]. Thickness and age of the sedimentary basin fill are measures of the amount of load-driven flexure of the lithosphere and the timing of uplift of the adjacent mountain range [*Jordan*, 1981; *Hagen et al*., 1985].

Isopach maps of the Powder River, Wind River, Green River, and Bighorn basins show that flexural loading of nearby ranges formed local foredeep depocenters in front of the range-bounding reverse faults during the early Cenozoic (Figure 2). Upper Paleocene and lower Eocene strata in the Powder River Basin thicken toward the eastern flank of the Bighorn Mountains [*Fox and Higley*, 1996]. Lower Eocene strata in the Wind River Basin thicken toward the Owl Creek and Bighorn Mountains to the northeast of the basin, with a greater sedimentation rate in the lower Eocene than in the Paleocene [*Keefer*, 1965]. Paleocene strata in the northeastern Green River Basin thicken toward the Wind River Range [*Carroll et al*., 2006], and lower Eocene strata in the southern Green River Basin thicken toward the Uinta Mountains [*Johnson and Andersen*, 2009, and references therein]. These observations suggest that although the segmentation of the Laramide intermontane basins was initiated during the latest Cretaceous [*Dickinson et al*., 1988], topographic loading of the Bighorn, Owl Creek, Wind River, and Uinta Mountains generated local depocenters mainly during the late Paleocene–early Eocene. Isopachs of lower Cenozoic strata in the Bighorn Basin also show thickening toward the Beartooth Mountains [*Parker and Jones*, 1986], but the lack of isopach maps for individual formations and deep erosion of the Eocene section at the surface [e.g., *Finn et al*., 2010] precludes a detailed evaluation of the subsidence during the early Cenozoic.

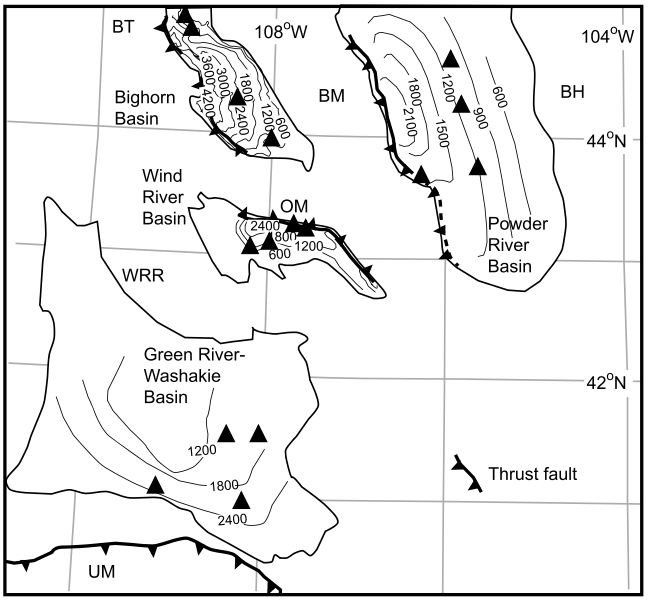

Figure 2. Isopachs of the late Paleocene–early Eocene strata in the Powder River, Bighorn, Wind River, and Green River basins. Contours are in 600 m. The isopachs of the Bighorn Basin and Powder River Basin include undifferentiated Fort Union Formation and Willwood/Wasatch Formation; isopach of the Wind River Basin is for the lower Eocene Wind River Formation, isopach of the Green River Basin is for the Paleocene–middle Eocene Fort Union, Wasatch, and Green River formations [*Keefer*, 1965; *Parker and Jones*, 1986; *Fox and Higley*, 1996; *Hoy and Ridgway*, 1997; *Johnson and Andersen*, 2009]. See Figure 1 for the abbreviations.

2.2. Basin Subsidence Curves

Basin subsidence curves were reconstructed based on the decompacted thickness of the Cretaceous–lower Cenozoic strata following *Angevine et al*. [1990] (Figure 3). The sediment load was removed following the method described by *Steckler and Watts* [1978]. Subsidence is calculated with respect to sea level. Because no generally accepted quantified curve of sea level exists and our study focuses on the comparison of contemporaneous subsidence rates in different basins, we have simply chosen to ignore sea-level changes and assume that they cause relatively low-magnitude variations in our calculated subsidence. We assigned water depths based on the lithofacies. Fluvial and lacustrine depositional environments are considered to have been at sea level, shale deposited in marine environments is considered to have been 300 m below sea level, and shaly sandstone deposited in marginal marine environments is considered to have been 100 m below sea level [*Angevine et al*., 1990]. We argue that such estimates introduce only small uncertainties to the amount of subsidence during the Cretaceous.

Tectonic subsidence histories of the Wind River and Green River basins show that the subsidence rate during the late Paleocene–early Eocene is clearly higher than during the Maastrichtian–late Paleocene, whereas the subsidence rate increase in the Powder River Basin is subtle (Figure 3). Two of the four studied wells in the Bighorn Basin show a subtle increase of subsidence rate, whereas the other two wells show a slight decrease of subsidence (Figure 3). Our reconstructed tectonic subsidence during the late Paleocene–early Eocene is a minimum because (1) accommodation space generated by topographic loading may not have been filled by sediment owing to the widespread exposure of the erosion-resistant Precambrian basement [*Carroll et al*., 2006; *Fan et al*., 2011a] as well as the late Paleocene–middle Eocene presence of many deep, large lakes, such as Lakes Gosiute in the Green River Basin, Waltman in the Wind River Basin, Uinta in the Uinta Basin, Belfry in the Bighorn Basin, and Lebo in the Powder River Basin [e.g., *Johnson*, 1985; *Yuretich*, 1989; *Carroll et al*., 2006], whose water depth could have exceeded 300 m [*Johnson*, 1985]; (2) the thickness of the preserved early Eocene strata is a minimum, because of post-depositional erosion; and (3) the estimate of post-early Eocene burial depth (1 km) for decompaction is a minimum, because of late Cenozoic erosion of post-Laramide basin fill [*McMillan et al*., 2006]. The estimate of burial depth is small compared to the 1–3 km thickness of post-laramide sedimentation based on fission track thermochronology of subsurface samples [*Pollastro and Barker*, 1984; *Beland*, 2002; *Peyton et al*., 2012]. Increased burial depth would increase the decompacted thickness of lower Eocene strata and the inferred magnitude of subsidence during the early Eocene. Although increased burial depth would also increase the decompacted thickness underlying the lower Eocene strata, the effect decreases rapidly as depth increases [*Angevine et al*., 1990]. Because the late Paleocene–early Eocene subsidence rates in Figure 3 are minimum rates, and the minimum subsidence rates of most of the studied wells are greater than the rates during Maastrichtian–late Paleocene time, we argue that the Laramide intermontane basins experienced accelerated subsidence during the late Paleocene–early Eocene.

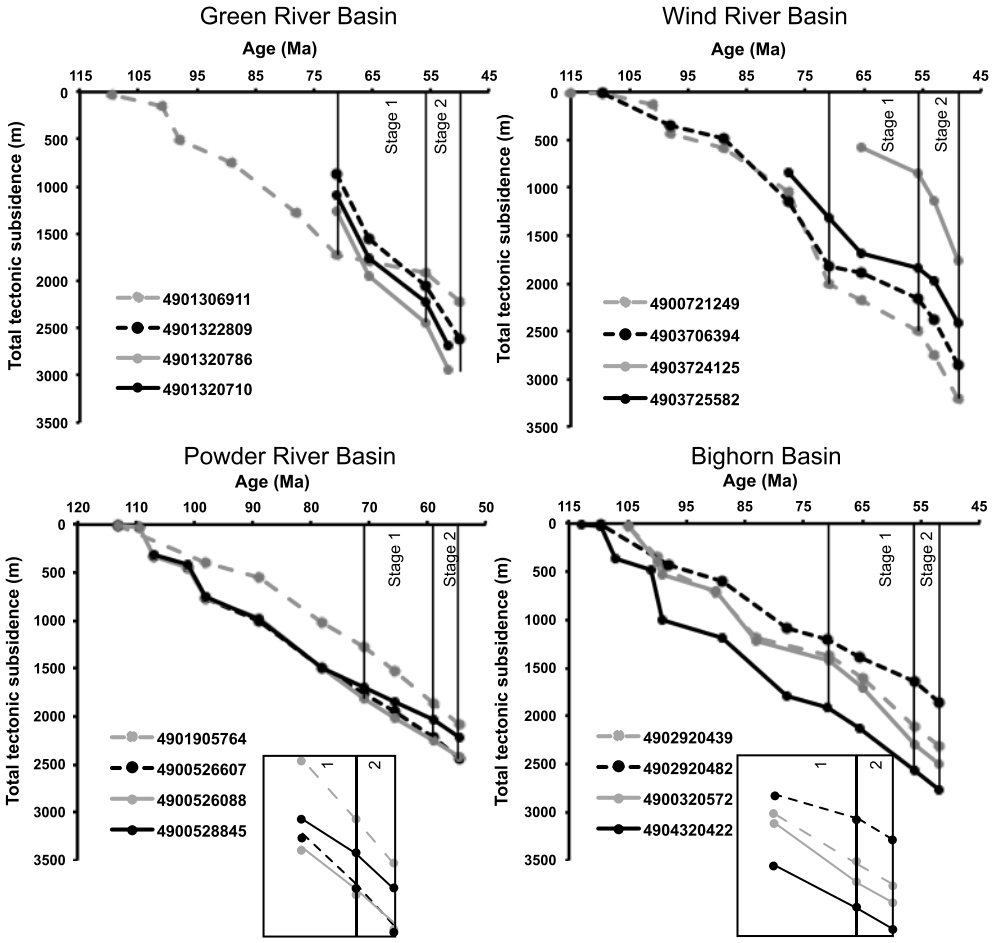

Figure 3. Tectonic subsidence curves of four studied localities in each basin. Locations of the studied localities are shown as triangles in Figure 2. Note the three wells in the Green River Basin (1322809, 1320786, and 1320710) do not have well tops older than the Maastrichtian, so we assigned pre-Maastrichtian subsidence values of 600 m, 800 m, and 1000 m for comparison with well 1306911. Subtle accelerations of subsidence rate in the Powder River and Bighorn basins are shown in small boxes. Note the late Paleocene–early Eocene subsidence rates in each basin are minimum rates. See text for discussion.

3. Surface Uplift of Laramide Mountain Ranges

3.1. Using Stable Isotopes to Reconstruct Paleoelevation

Paleoelevation reconstructions of the Laramide mountain ranges are based on stable isotope paleoaltimetry and paleobotanical studies [*Norris et al.*, 1996; *Wolfe et al.*, 1998; *Dettman and Lohmann*, 2000; *Fricke*, 2003; *Fan and Dettman*, 2009; *Fan et al.*, 2011a]. Such reconstructions rely on comparing ancient surface water stable isotopic composition or fossil leaf physiognomy to a modeled or empirical relationship with elevation [e.g., *Wolfe et al.*, 1998; *Quade et al.*, 2007; *Rowley*, 2007]. Four types of carbonate materials are typically used for paleoelevation studies in this region, including paleosol carbonates, mammal tooth enamel, freshwater bivalves, and early diagenetic cements. Because the $\delta^{18}O$ values of paleosol carbonates reflect the $\delta^{18}O$ values of local basinal precipitation [e.g., *Quade et al.*, 2007], and the $\delta^{18}O$ values of the early Eocene surface water reconstructed from mammal teeth enamel in *Fricke* [2003] are similar to the $\delta^{18}O$ values of late Paleocene–early Eocene rivers charged by basinal precipitation [*Fan and Dettman*, 2009], the two type of materials do not give paleoevation information of the basin-bounding mountains. Here we focus exclusively on the oxygen isotope results of freshwater bivalve fossils and early diagenetic fluvial/lacustrine carbonate cement that were formed under equilibrium with water derived from mountain ranges in order to reconstruct the paleoelevation of the mountain ranges (Table 1 and Figure 4) [*Norris et al.*, 1996; *Dettman and Lohmann*, 2000; *Davis et al.*, 2008; *Fan and Dettman*, 2009; *Fan*

Table 1. Compiled Stable Isotope and Leaf Physiognomy Results and Estimated Paleoelevation of Major Laramide Mountain Ranges

Laramide Ranges	Studied Carbonate Type	Age (Ma)	Lowest Carbonate δ^{18}O (PDB)	Calculated Water δ^{18}O (SMOW)[a]	Mean Catchment Paleoelevation (km)[b]	References
Black Hills	Bivalve aragonite	58–54	−21.3	−22.8	>2	*Fan and Dettman* [2009]
Bighorn Mountains	Bivalve aragonite	58–54	−21.3	−22.8	>2	*Fan and Dettman* [2009]
Beartooth Mountains	Bivalve aragonite	59–54	−12.6	−13.0	<2	*Fan and Dettman* [2009]
Wind River and Washakie ranges	Fluvial calcite cement	53.5–51	−17.6	−16.7	>2	*Fan et al.* [2011a]
Owl Creek Mountains	Fluvial calcite cement	60–55.5	−13.1	−12.2	<2	*Chamberlain et al.* [2012]
Owl Creek Mountains	Fluvial calcite cement	55.5–51	−20.8	−19.9	>2	*Chamberlain et al.* [2012]
Uinta Mountains	Fluvial calcite cement	53–52	−9.3	−8.4	<2	*Davis et al.* [2008]
Uinta Mountains	Bivalve aragonite	53–52	−9.3	−8.7	<2	*Fan and Dettman* [2009]
Uinta Mountains	Lacustrine calcite cement	50	−16.0	−15.1	>2	*Norris et al.* [1996]
Uinta Mountains	Fossil leaf	45			~3	*Wolfe et al.* [1998]

[a]Water δ^{18}O values are calculated from bivalve aragonite and calcite cement. See text for details of calculation.
[b]Paleoelevation reconstruction is based on the relationship of modern precipitation δ^{18}O values versus elevation presented in Figure 4a.

et al., 2011a; *Chamberlain et al.*, 2012]. Freshwater bivalve aragonite and early diagenetic fluvial/lacustrine carbonate are formed in equilibrium with river and lake water, which could be charged by surface runoff or groundwater derived from basin-bounding mountain ranges. The contribution of lowland precipitation to these rivers and lakes was small compared to the highland surface runoff or groundwater because the δ^{18}O values of these carbonates are lower than those of paleosol carbonates [*Koch et al.*, 1995; *Fan et al.*, 2011a]. Therefore, the δ^{18}O values of these carbonates mainly reflect the δ^{18}O values of precipitation in the highland and can be used to constrain the mean catchment paleoelevation of the mountain ranges [*Rowley*, 2007]. Paleoelevation reconstructed using leaf physiognomy is also summarized here, because it reflects mean catchment elevation [*Wolfe et al.*, 1998].

Possible factors affecting the interpretation of the δ^{18}O values of river and open lake water in the Rocky Mountains include diagenesis, evaporation and snow sublimation, latitude change, temperature, source water δ^{18}O values, water vapor source, precipitation amount, drainage reorganization, and elevation [e.g., *Morrill and Koch*, 2002; *Lee and Fung*, 2008; *Lechler and Niemi*, 2011a]. Evaluation of the studied carbonates [*Norris et al.*, 1996; *Dettman and Lohmann*, 2000; *Davis et al.*, 2008; *Fan and Dettman*, 2009; *Fan et al.*, 2011a; *Chamberlain et al.*, 2012] shows that the oxygen isotope composition did not experience late-stage digenetic influence. Our compiled isotope data refer to rivers and hydrologically open lake water; thus, we neglect the effect of evaporation because evaporation for such waters should be small, especially in the humid paleoclimate of the early Cenozoic [e.g., *Wilf*, 2000; *Hyland et al.*, 2013]. Recent studies have shown that drainage reorganization may change the source water and thus the δ^{18}O values of river and lake water [*Carroll et al.*, 2008; *Davis et al.*, 2008, 2009]. However, our studied period in the Green River Basin predates the timing of major drainage reorganization [*Carroll et al.*, 2008; *Davis et al.*, 2008]. Drainage reorganization is unlikely to have occurred in the other three basins as well because sedimentological data, paleoflow directions, and paleogeographic reconstructions based on sandstone body geometries have shown that the paleorivers in these basins were derived from the local Laramide highlands during the late Paleocene–early Eocene [e.g., *Winterfeld and Conard*, 1983; *Flores and Ethridge*, 1985; *Crews and Ethridge*, 1993; *Hoy and Ridgway*, 1997; *Carroll et al.*, 2006; *Fan et al.*, 2011a, 2011b]. Snowpacks are isotopically altered by snow sublimation and the snowmelt is $_{18}$O-enriched; hence, the river and lake water charged by the snowmelt is also $_{18}$O-enriched. Such enrichment is altitude dependent because high-elevation snowpacks are sustained longer into the melt season and experience increased sublimation-induced $_{18}$O-enrichment [*Lechler and Niemi*, 2011a]. Because climate was warm and wet during the early Cenozoic [e.g., *Wilf*, 2000; *Zachos et al.*, 2001; *Fricke and Wing*, 2004; *Wing et al.*, 2005; *Sewall and Sloan*, 2006; *Fricke et al.*, 2010; *Snell et al.*, 2013; *Hyland et al.*, 2013], the influence of snow sublimation should be negligible. The paleolatitude of the study area was ~6°N of today, and the latitude difference caused the ancient surface water δ^{18}O values to be ~2‰ lower than today [*Fan and Dettman*, 2009]. The δ^{18}O value of seawater was ~1‰ lower than that of modern seawater due to smaller global ice volume during the early Cenozoic [*Zachos et al.*, 1994]. However, the influence of latitude shift and global ice volume (~3‰) may be canceled out by temperature.

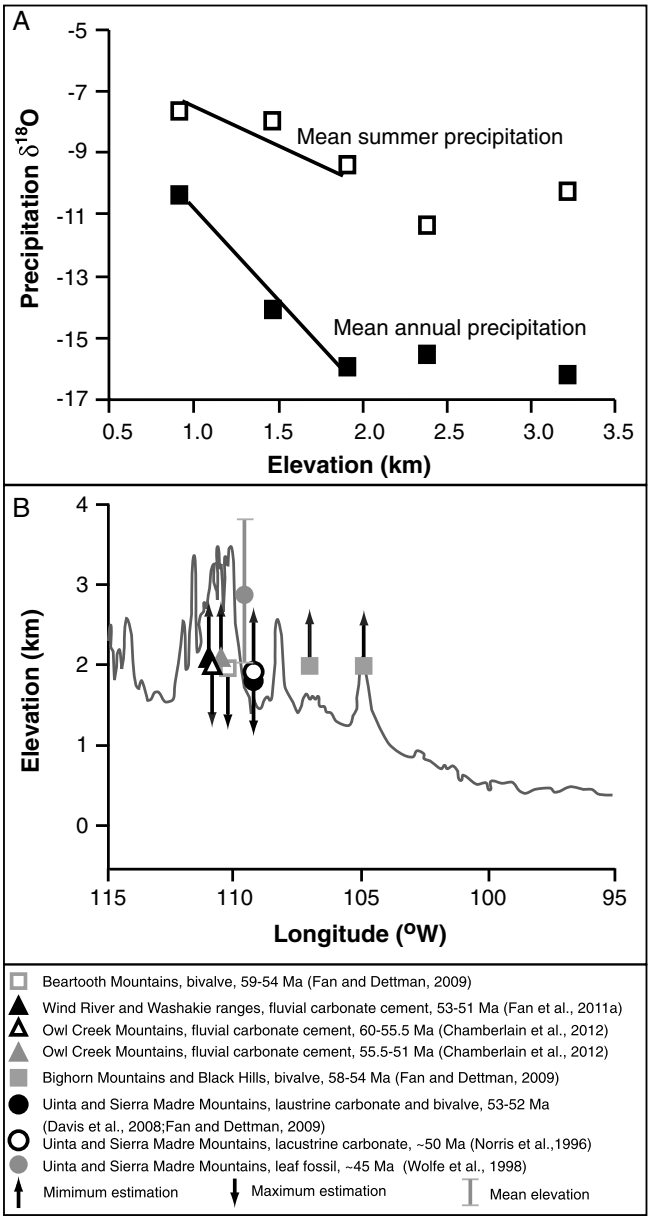

Figure 4. (a) Modern mean annual and summer precipitation δ^{18}O values [*Vachon et al.*, 2010, WY06, WY08, WY95, WY99, NE99] along a W-E transect across Wyoming and Nebraska; (b) reconstructed late Paleocene–early Eocene paleoelevation compared to modern elevation profile along 43°N (gray line). See text and Table 1 for paleoelevation estimates and references.

Temperature influences both the isotope fractionation between water and carbonate, and during vapor condensation. River water δ^{18}O values are determined from shell aragonite δ^{18}O values by using an empirically determined relationship [*Kohn and Dettman*, 2007]. River and lake water δ^{18}O values are calculated from calcite cement by using the oxygen isotope fractionation relationship between calcite and water [*Kim and O'Neil*, 1997] and temperature of 18°C. This temperature is the late Paleocene–early Eocene mean annual air temperature based on paleobotanical and oxygen isotope estimates in the Bighorn, Green River, Powder River, and Wind River basins [*Fricke and Wing*, 2004; *Wing et al.*, 2005] and is consistent with the growth temperature of early Eocene calcite cement in the Colorado Plateau [*Huntington et al.*, 2011]. This temperature is ~12°C higher than modern mean annual temperature and may have caused the precipitation δ^{18}O values to be ~3‰ higher than modern precipitation δ^{18}O values.

Modern climate for our study area is influenced by three air masses that originate over the Arctic, the Gulf of Mexico/Atlantic Ocean, and the Pacific Ocean, and precipitation biases to summer season [*Bryson and Hare*, 1974; *Z. Liu et al.*, 2010]. Southward displacement of the winter jet stream brings moist Pacific air mass to the western United States during the winter, and the amount of precipitation decreases as the vapor moves inland eastward [*Z. Liu et al.*, 2010]. Arctic air mass is dry and the influence of precipitation on isotope values in the study area is small. Summer precipitation from the Gulf of Mexico/Atlantic Ocean decreases as elevation and continentality increase toward the Rocky Mountain front [*Z. Liu et al.*, 2010]. Prior to the early Cenozoic, the development of the Sevier fold-and-thrust belt caused significant shortening and thickening, forming a high-elevation hinterland plateau [*DeCelles*, 2004]. This high topography may have blocked moisture from the Pacific Ocean because there was significant paleovalley incision and braided river aggradation in California and Nevada during the early Cenozoic [*Cassel et al.*, 2012]. In addition, warm climate during the early Cenozoic [e.g., *Zachos et al.*, 2001; *Fricke and Wing*, 2004; *Wing et al.*, 2005; *Snell et al.*, 2013; *Hyland et al.*, 2013] may have limited the southward displacement of winter jet stream and reduced the vapor input from the Pacific Ocean. On the other hand, the Mississippi Embayment was ~5° farther north relative to its current location, and moisture from the Atlantic Ocean brings relatively abundant summer rainfall into the study area [*Sewall and Sloan*, 2006].

Ocean-derived precipitation with minimal effects of continentality should lead to higher $\delta^{18}O$ values of precipitation in the study area. However, precipitation during the Paleocene-Eocene was 4–10 times higher than it is today [*Retallack*, 2005; *Sewall and Sloan*, 2006], and high precipitation may reduce $\delta^{18}O$ values of rainfall due to amount effect [*Dansgaard*, 1964]. Although the influence of these two factors on our reconstructed surface water $\delta^{18}O$ values and paleoelevation reconstruction cannot be easily resolved, a comparison of Paleocene-Eocene precipitation with modern precipitation near the Gulf of Mexico may offer some insights. The $\delta^{18}O$ values of the Paleocene-Eocene paleosol carbonates formed under least evaporative conditions near the Gulf of Mexico are approximately $-5‰$ [*White*, 2005], and the calculated precipitation $\delta^{18}O$ value is ~0.5‰ using a carbonate formation temperature of ~41°C. This high temperature is based on a clumped isotope study showing that pedogenic carbonate formation temperature is ~18°C higher than mean annual temperature [*Snell et al*., 2013], and a mild temperature gradient (~0.4°C/°latitude) in the early Eocene is assumed [*Fricke and Wing*, 2004]. The calculated precipitation $\delta^{18}O$ value is associated with warm season (most likely summer) precipitation $\delta^{18}O$ values because soil carbonates form during warm season [*Passey et al*., 2010; *Snell et al*., 2013; *Hough et al*., 2014]. The Paleocene-Eocene warm season precipitation $\delta^{18}O$ value is about 3‰ higher than the modern summer river water $\delta^{18}O$ values of Pecos River near Langtry, TX, and Devils River near Comstock, TX, which have an elevation of ~1 km [*Coplen and Kendall*, 2000]. Because the 3‰ difference can be explained by elevation difference alone, it is possible that the influence of dominant vapor from the Gulf of Mexico may cancel out the influence of high precipitation amount on precipitation $\delta^{18}O$ values in the study area during the Paleocene-Eocene.

We reconstruct paleoelevations by comparing the reconstructed surface water $\delta^{18}O$ value with modern precipitation $\delta^{18}O$ values. Five stations in Wyoming and Nebraska [*Vachon et al*., 2010] show that (1) modern mean annual $\delta^{18}O$ values are correlated with elevation when the elevation is below ~2 km and (2) modern mean annual precipitation $\delta^{18}O$ values at elevations of ~2 km or above are equal to or less than approximately $-15‰$ (Figure 4a). Therefore, we assume that when the ancient mean surface water $\delta^{18}O$ value is lower than $-15‰$, the range that provided precipitation into the studied rivers and lakes had a mean catchment elevation higher than 2 km; otherwise, the catchment elevation is inferred to have been less than 2 km (Figure 4b). Other possible causes for surface water with $\delta^{18}O$ values lower than $-15‰$ in catchments lower than 2 km include large contributions of precipitation from the $_{18}O$-depleted Artic air masses, or $_{18}O$-depleted vapors passing the high Sevier hinterland [*DeCelles*, 2004; *Snell et al*., 2014]. However, both scenarios are unlikely given that Arctic air masses shifted northward during warm periods [*Z. Liu et al*., 2010], and only a limited amount of vapor can pass the high Sevier hinterland. In addition, warm global temperatures and northward invasion of the Mississippi embayment may have promoted a strong summer monsoon, advecting water vapor from the $_{18}O$-enriched Gulf of Mexico [*Sewall and Sloan*, 2006; *Fricke et al*., 2010]. Therefore, the cutoff of $-15‰$ may be a lower estimate, leading to conservative paleoelevation estimation for the mountain ranges. The lapse rate of modern precipitation $\delta^{18}O$ values displays large uncertainties in the western United States [e.g., *Lechler and Niemi*, 2011b] and introduces large uncertainty into paleoelevation estimates. Here we do not use the lapse rate for absolute paleoelevation reconstruction.

3.2. Results

The attainment of high elevation of Laramide ranges seems to follow a trend from northeast to southwest (Figure 5). The earliest signal of ancient river water with the lowest $\delta^{18}O$ values ($-23‰$) occurred in the Powder River Basin in northeast Wyoming during the late Paleocene (~58 Ma), suggesting that the river water originated in the highlands of the Bighorn Mountains with an elevation of >2 km, perhaps as high as 4.5 ± 1.3 km [*Fan and Dettman*, 2009]. Also, large seasonal isotopic variations show that the ancient river was seasonally charged by highland snowmelt and precipitation in basinal lowlands [*Fan and Dettman*, 2009]. The $\delta^{18}O$ values of ground water in the northwestern corner of the Wind River Basin in central Wyoming was as low as $-17‰$ during the early Eocene (~55.5–51 Ma), suggesting that groundwater was sourced from the highlands of the Wind River Range and Washakie Range (>2 km high) [*Fan et al*., 2011a]. This is additionally supported by the finding that the lowest $\delta^{18}O$ values of groundwater in the northern Wind River Basin were approximately $-12‰$ during the Paleocene but changed to ~ $-20‰$ in the early Eocene [*Chamberlain et al*., 2012]. Groundwater in the northern Wind River Basin may be sourced from the highlands of the Owl Creek

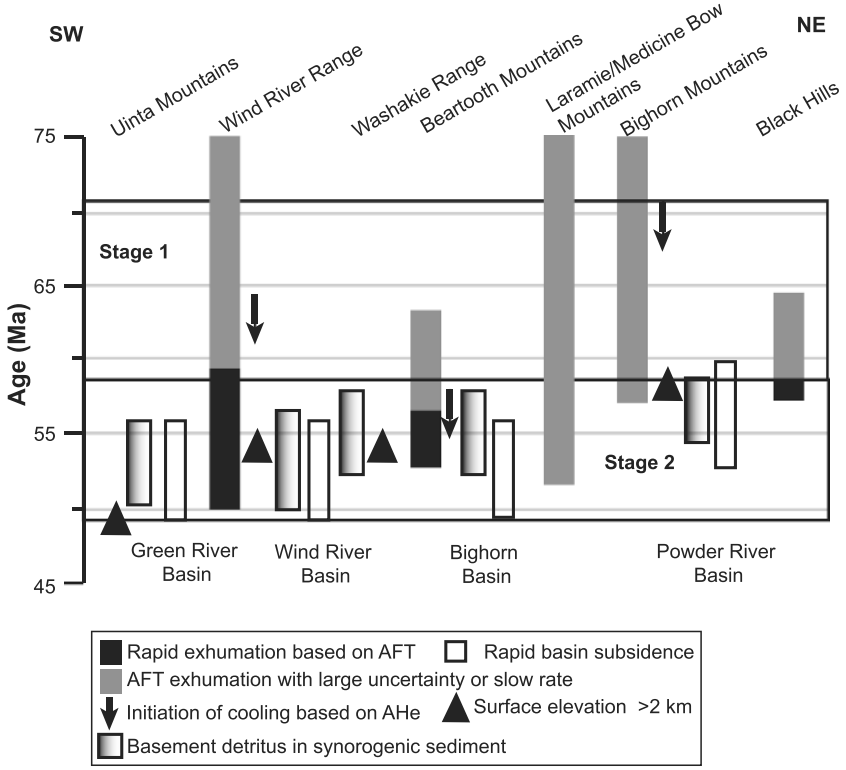

Figure 5. Timing of fast exhumation and major surface elevation gain of major Laramide ranges and subsidence of major intermontane basins across Wyoming. See text and Figure 1 for data references.

Mountains. The $\delta^{18}O$ values of river water or fresh lake water, reconstructed from freshwater bivalve fossils and lacustrine carbonate cement, were as high as approximately −8‰ at 53–52 Ma in the Green River Basin [*Davis et al.*, 2008; *Fan and Dettman*, 2009], suggesting that high elevation of the Uinta Mountains was not attained until ~50 Ma, when the $\delta^{18}O$ values of lake water reconstructed from lacustrine carbonate decreased to −15‰ [*Norris et al.*, 1996]. This inference of elevation is consistent with the leaf physiognomic reconstruction of mean catchment elevation of ~3 km during the early middle Eocene [*Wolfe et al.*, 1998]. The $\delta^{18}O$ values of river water reconstructed from freshwater bivalve fossils in the Bighorn Basin was as low as −13‰ during the late Paleocene and earliest Eocene [*Fan and Dettman*, 2009], suggesting that the Beartooth Mountains attained elevations higher than 2 km after the earliest Eocene.

4. Exhumation of Laramide Ranges

4.1. Thermochronological Data

Apatite fission-track (AFT) and apatite (U-Th)/He (AHe) ages record the time when the analyzed mineral passed through the temperature window of ~120–60°C for AFT [e.g., *Gallagher et al.*, 1998] and of ~80–40°C for AHe [e.g., *Farley*, 2002]. Low-temperature thermochronology when applied to basement samples collected at different elevations following the most direct and steepest path possible, whereby changes in elevation are assumed to represent changes in the distance traveled from the closure temperature window, provides information on the thermal history of a specific range [e.g., *Fitzgerald et al.*, 1995; *Peyton et al.*, 2012]. Exhumation ages of Laramide mountain ranges from topographic profiles within Precambrian crystalline rocks mainly vary between Campanian and early Eocene, with rapid cooling clustering around the late Paleocene–early Eocene (Figure 5). *Strecker's* [1996] AFT study of the Black Hills shows that exhumation rate was slower during the early Paleocene, accelerated at ~58 Ma, and peaked shortly after ~55 Ma. New AFT data from the Bighorn Mountains indicate an increase in exhumation rate between ~99 and ~57 Ma [*Peyton et al.*, 2012]. AFT data from the Wind River Range show that cooling may have initiated as early as ~85 Ma [*Cerveny and Steidtmann*, 1993], and new best fit AFT modeling from this study based on data

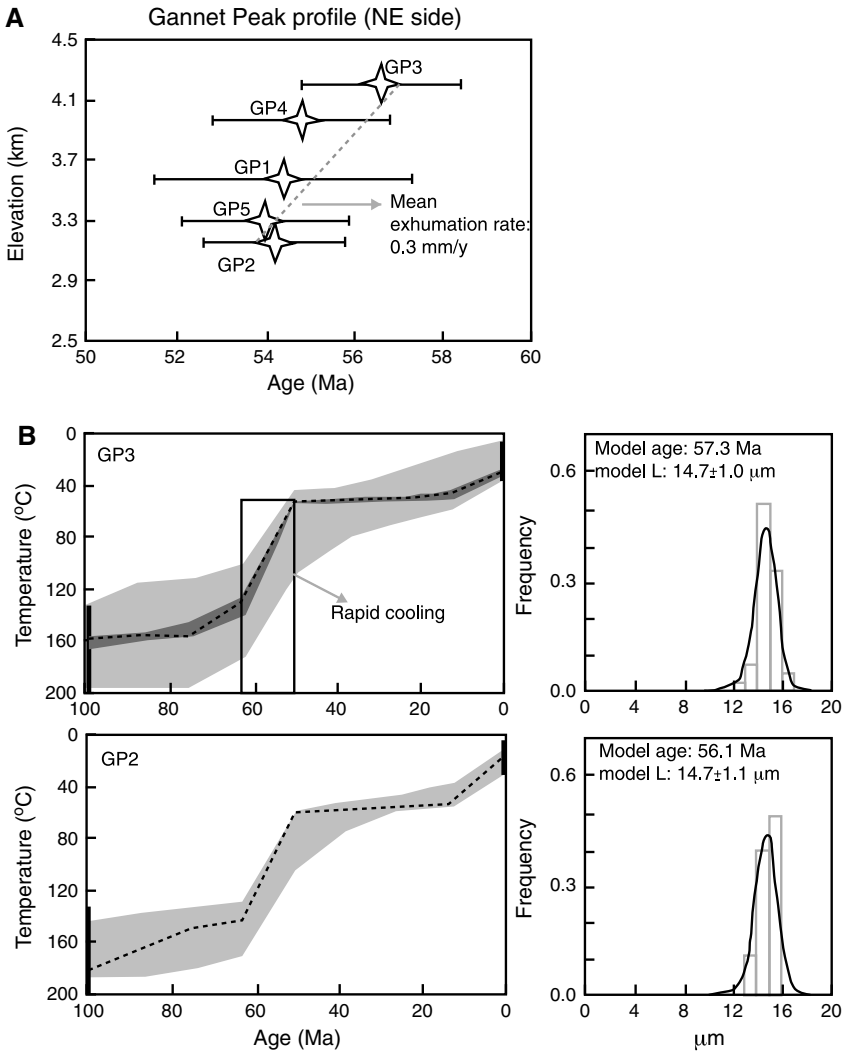

Figure 6. (a) Plot of AFT age versus elevation for basement samples collected from the northeastern side of Gannet Peak in the Wind River Range. (b) AFTSolve [*Ketcham et al.*, 1999] thermal modeling of samples GP3 and GP2 (4208m; 3298m); data are from *Peyton et al.*, 2012. The model was initiated at 100 Ma with temperature equals 200°C; an additional constraint was applied between 40 and 10°C at present. Lengths reported are corrected for *c* axis for modeling purposes. The light gray area corresponds to the acceptable fit, the dark gray area to the good fit, and the dashed black line to the best fit.

from a topographic profile on Gannett Peak [*Peyton et al.*, 2012] shows that faster cooling occurred at ~65–50 Ma and was followed by a sharp decrease in cooling rate after ~50 Ma (Figure 6). This decrease can be interpreted as the result of removal of Phanerozoic strata (~55 Ma) followed by exposure of more resistant crystalline basement. Similar studies of the Beartooth Mountains show that cooling commenced during the early Paleocene and possibly earlier, and that rapid exhumation started at ~57 Ma [*Omar et al.*, 1994]. However, AFT data from the Granite, Ferris, Seminoe, Shirley, Elk, and Rawlins Mountains in southeastern Wyoming show a large span of ages between 146 Ma and 29 Ma with a large Paleocene component [*LeFebre*, 1988]. AFT data from the Laramie and Medicine Bow Mountains show ages between 79 Ma and 52 Ma [*Cerveny*, 1990; *Kelley*, 2005]. This clear discrepancy in age of exhumation may be caused by thermal perturbation associated with magmatism in the Colorado Mineral Belt, which may have been largely influenced by small-scale asthenosphere upwelling during the flat slab insertion [*Jones et al.*, 2011], prolonged cooling and exhumation history of these ranges during the transition from east–west shortening to south–north shortening [*Gries*, 1983], and the opening of the Rio Grande Rift during the late Cenozoic [*Moucha et al.*, 2008].

Although the lower temperature range of the AHe thermochronometer would seem to make this technique ideal for elucidating shallower crustal processes compared to AFT, its application to several Laramide ranges is compromised by the strong effect of radiation damage on He diffusivity [*Peyton et al*., 2012]. Best fit time-temperature paths derived from the AHe data show that cooling initiated in the Bighorn Mountains before ~71 Ma, in the Wind River Range before ~66 Ma, and in the Beartooth Mountains before ~58 Ma [*Crowley et al*., 2002; *Peyton and Carrapa*, 2013]. Results of AHe modeling of these new ages are generally consistent with AFT data [*Peyton et al*., 2012]. The summarized thermochronology data display large variations and a distinct exhumation pattern cannot be observed.

4.2. Provenance Data

Upper Paleocene–lower Eocene synorogenic conglomerates along the flanks of several Laramide uplifts show an up-section change from predominantly Paleozoic carbonate clasts to Precambrian basement clasts, documenting erosional exhumation of the neighboring Laramide ranges [*Winterfeld and Conard*, 1983; *DeCelles et al*., 1991; *Steidtmann and Middleton*, 1991; *Crews and Ethridge*, 1993; *Hoy and Ridgway*, 1997; *Carroll et al*., 2006; *Fan et al*., 2011a]. During the late Paleocene and early Eocene, the upper member of the Fort Union Formation and the Kingsbury and Moncrief Conglomerates in the Powder River Basin record rapid erosion of the Bighorn Mountains [*Hoy and Ridgway*, 1997], and the Beartooth Conglomerate in the northwestern Bighorn Basin records rapid erosion and structural growth of the Beartooth Mountains [*DeCelles et al*., 1991]. The early Eocene Indian Meadows Formation records erosion of the Washakie Range, the early Eocene Wind River Formation and Cathedral Bluffs Tongue of the Wasatch Formation record erosion of the Wind River Range, and the Richards Mountain Conglomerate records the erosion of the Uinta Mountains during the early Eocene [*Winterfeld and Conard*, 1983; *Steidtmann and Middleton*, 1991; *Crews and Ethridge*, 1993; *Fan et al*., 2011a]. Widespread basement erosion in these Laramide ranges did not take place until the late Paleocene–early Eocene, as basement clasts are rare in pre–late Paleocene conglomerates [*Carroll et al*., 2006, and references therein].

Detrital geochemical and geochronological data support the argument that widespread erosion of crystalline basement in Laramide ranges occurred during the early Eocene [*Fan et al*., 2011a, 2011b]. Precambrian crystalline basement rocks in Wyoming have high $^{87}Sr/^{86}Sr$ ratios (>0.711) compared to Phanerozoic sedimentary rocks, whose low $^{87}Sr/^{86}Sr$ ratios (<0.711) are dominated by Phanerozoic marine carbonate. The $^{87}Sr/^{86}Sr$ ratios of early Eocene river water in the Green River and Powder River basins, reconstructed from the $^{87}Sr/^{86}Sr$ ratios of freshwater bivalve fossils, are higher than 0.711 [*Fan et al*., 2011b]. These high values suggest that Phanerozoic marine carbonate was not the dominant river catchment lithology during the early Eocene and that the Laramide ranges surrounding the two basins, including the Wind River Range, Sierra Madre Range, Uinta Mountains, Bighorn Mountains, and Black Hills were exhumed to the level of Precambrian basement rocks before early Eocene time [*Fan et al*., 2011b]. The early Eocene Wind River Formation contains ~20% Archean zircons, consistent with the percentage of Archean zircons found in modern river sands derived from the Wind River Range with large basement rock exposure in river catchments. This set of observations suggests erosional exhumation of Archean basement rocks in the Wind River and Washakie ranges during the early Eocene [*Fan et al*., 2011a].

5. Discussion

5.1. Multistage Development of Laramide Deformation

Although there are lines of evidence suggesting that Laramide deformation initiated during the Middle and Late Cretaceous [e.g., *Merewether and Cobban*, 1986; *Schwartz and DeCelles*, 1988; *Steidtmann and Middleton*, 1991], it is commonly accepted that the bulk of the deformation initiated during the early Maastrichtian (~71 Ma) [*Chapin and Cather*, 1983; *Gries*, 1983; *Dickinson et al*., 1988; *Chapin and Cather*, 1990]. This inference is based on the termination of marine sedimentation and initiation of coastal plain-marginal marine environments during the deposition of the Lance and Fox Hills formations before the predominant continental environments during Cenozoic time [*Dickinson et al*., 1988]. The onset of Laramide deformation also is slightly younger than the timing of interruption of arc magmatism in the southern California segment of the Cordilleran arc [*Saleeby*, 2003] and is consistent with concomitant eastward migration of the magmatic front, which is postulated to have been caused by low-angle subduction of the Farallon plate [e.g., *Livaccari et al*., 1981; *Constenius*, 1996], and with the timing of initiating flat subduction modeled by reverse mantle convection

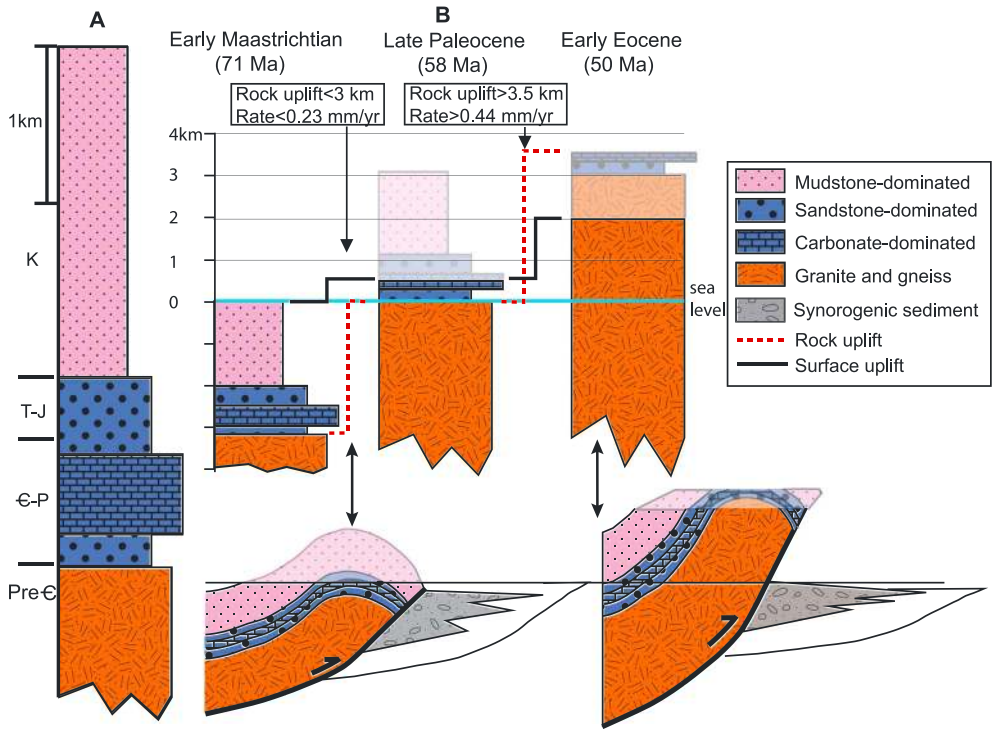

Figure 7. (a) General stratigraphy in central Wyoming (modified from *Keefer* [1970]). (b) Schematic diagram illustrating surface uplift and exhumation during the two stages of Laramide deformation. Wind River Range is used as an example. The transparent area represents erosion, which equals exhumation.

[*Liu et al.*, 2008]. Regardless of whether we consider Laramide deformation to have started in the middle or Late Cretaceous, the foregoing summary of basin subsidence, surface uplift, and exhumation shows that during the Maastrichtian-Paleocene, both surface and rock uplift rate were lower compared to those of the late Paleocene–early Eocene in Wyoming. Our data set also shows that Laramide intermontane basins in Wyoming experienced faster subsidence, and the ranges were exhumed to current elevations with Precambrian basement erosion by the early Eocene. The current data suggest that Laramide deformation is characterized by two stages of deformation and exhumation: Maastrichtian–late Paleocene (~71–58 Ma, stage 1) and late Paleocene–early Eocene (~58–50 Ma, stage 2). This two-stage history model is consistent with the timing of Laramide structural deformation and sedimentation in the Rocky Mountain area and Colorado Plateau summarized by *Gries* [1983] and *Chapin and Cather* [1983].

5.2. Late Paleocene–early Eocene Accelerated Laramide Deformation

The amount and rate of rock uplift of Laramide ranges during the two stages can be reconstructed by combining data of regional stratigraphic cover thickness and chronology with paleoelevation and erosional exhumation data. Here we use the Wind River Range as an example to demonstrate the rationale (Figure 7); the reconstructed amounts and rates of rock uplift of major Laramide ranges are summarized in Table 2 assuming that rock uplift is equal to surface uplift plus exhumation [*England and Molnar*, 1990]. The thickness of the Paleozoic and Mesozoic strata is ~3.4 km in the Wind River Range [*Keefer*, 1970]. During the early Maastrichtian, coastal plain–marginal marine environments near sea level controlled sedimentation in Wyoming. Thus, we assume that regional elevation was near sea level (~0 km) at that time and that the boundary between the Precambrian basement and Phanerozoic sedimentary cover was ~3.4 km below sea level. By the late Paleocene, reverse faults had deformed Cretaceous strata, increased topographic relief and the depth of erosion, and the Laramide ranges had ~0.5 km of topographic relief based on restored balanced cross sections and reconstructed levels of erosion in Laramide ranges [e.g., *DeCelles et al.*, 1991; *Hoy and Ridgway*, 1997]. This low elevation estimate is consistent with the fact that ~2.9 km of nonresistant Mesozoic and Upper Paleozoic shale and sandstone had to be eroded before any resistant, gravel-producing Paleozoic

AGU Tectonics

Table 2. Compiled Stratigraphic Thicknesses and Timing of Changing Predominant Detritus Type and Calculated Amounts and Rates of Rock Uplift

Laramide Range	M (m)[a]	UP (m)[b]	LP (m)[c]	Earliest Predominant Limestone Detritus	Age (Ma)	Earliest Basement Detritus >30%	Age (Ma)	Time of High Elevation (Ma)[d]	Stage 1: Max RU (m)[e]	Stage 1: Max Rate of RU (mm/yr)[f]	Stage 2: Min RU (m)[g]	Stage 2: Min. Rate of RU (mm/yr)[h]	References
Bighorn Mountains	2500	200	600	Upper Tongue River Member	60	Base of Wasatch Fm. and Moncrief Conglomerate	53	58	3300	0.30	3000	0.43	*Hose* [1955]; *Whipkey et al.* [1991]; *Hoy and Ridgway* [1997]
Uinta Mountains	3700	550	500	Base of Richards Mountains Conglomerate	55	Upper Richards Mountains Conglomerate	53	50	4750	0.30	3000	0.60	*Crews and Ethridge* [1993]; *Sprinkel* [2000]
Wind River Range	2600	250	500	Upper Fort Union Fm.	60	Base of Wind River Fm.	52	52	3350	0.30	3000	0.38	*Courdin and Hubert* [1969]; *Keefer* [1970]; *Fan et al.* [2011a]
Washakie/Owl Creek ranges	1600	150	600	Upper Fort Union Fm.	60	Base of Wind River Fm.	52	52	2350	0.21	3000	0.38	*Berry and Littleton* [1961]; *Courdin and Hubert* [1969]; *Fan et al.* [2011a]
Beartooth Mountains	2500	150	900	Base of Beartooth Conglomerate	60	Lower Willwood Fm./upper Beartooth Conglomerate	55	<54	3550	0.32	3000	_[i]	*Wise* [1957]; *DeCelles et al.* [1991]

[a]Mesozoic is siliciclastic-dominated.
[b]Upper Paleozoic (UP) is siliciclastic-dominated.
[c]Lower Paleozoic (LP) is carbonate-dominated.
[d]See Table 1 for references.
[e]Maximum mount of rock uplift (RU) is calculated as the sum of the thickness of Mesozoic and Upper Paleozoic (exhumation) plus the thickness of Lower Paleozoic (surface uplift).
[f]Maximum rate of rock uplift (RU) is calculated as the maximum amount of rock uplift divided by the difference of 71 Ma (start of Maastrichtian) and the age of earliest predominant limestone detritus.
[g]Minimum amount of rock uplift (RU) is calculated as the sum of the thickness of Lower Paleozoic and 1 km of basement (exhumation) plus the difference between 2 km and the thickness of Lower Paleozoic (surface uplift).
[h]Minimum rate of rock uplift (RU) is calculated as the minimum amount of rock uplift divided by the age difference between the earliest predominant limestone detritus and the smaller age of documented high elevation and earliest basement detritus >30%.
[i]Rate of rock uplift cannot be calculated because the timing of attaining high elevation of the Bighorn Mountains is not documented.

10.1002/2012TC003221

carbonate and Precambrian basement could have been exposed on the top of Laramide structures [*DeCelles et al*., 1991; *Carroll et al*., 2006]. The thickness of the resistant Paleozoic carbonate in the Wind River Range is ~0.5 km [*Keefer*, 1970], which can be assumed to be the main unit that produced topography and thus the paleoelevation of the mountains during the early Paleocene. Therefore, by the end of stage 1, about 2.9 km of Mesozoic and Upper Paleozoic rocks had been eroded from the crests of the Wind River Range. The total estimated amount of erosion (~2.9 km) is a maximum because the lower Mesozoic strata may be not completely eroded during the Maastrichtian-Paleocene, as indicated by the high abundance (>50%) of quartz and siltstone/shale rock fragments (~30%) in the upper Fort Union Formation and Indian Meadows Formation [*Courdin and Hubert*, 1969; *Fan et al*., 2011a], and because the Laramide mountain ranges may have experienced pre-Laramide exhumation [e.g., *Merewether and Cobban*, 1986; *Steidtmann and Middleton*, 1991]. Paleoelevations of the Wind River Range indicate surface uplift from near sea level to ~0.5 km by the late Paleocene, which is also a maximum estimate. Therefore, the Wind River Range experienced maximum rock uplift of ~3.4 km at a rate of ~0.30 mm/yr between ~71 Ma and ~60 Ma. Similar calculations for the Uinta, Beartooth, Bighorn, and Owl Creek/Washakie mountains yield maximum rock uplift of 2.3–4.8 km and maximum rate of rock uplift of 0.21–0.32 mm/yr during stage 1 (Table 2).

The reconstructed average paleoelevation of the Wind River Range was >2 km (most likely 3.5 km) during the late Paleocene–early Eocene [*Fan et al*., 2011a], suggesting that surface uplift was > ~1.5 km during stage 2. Erosion of Precambrian basement rocks provided most of the arkosic detritus that was deposited in the Wind River Basin [*Courdin and Hubert*, 1969; *Fan et al*., 2011a]. The deposited basement clasts require more than 1.5 km of erosion of the Lower Paleozoic rocks (with stratigraphic thickness of ~0.5 km) and Precambrian basement (with stratigraphic thickness larger than 1 km). Our estimate of basement erosion (1 km) is most likely a minimum because basement-derived boulders and cobbles are widespread in the Wind River Basin [*Courdin and Hubert*, 1969; *Keefer*, 1970; *Fan et al*., 2011a], and the late Paleocene and early Eocene was warm and humid, possibly intensifying physical and chemical weathering [*Smith et al*., 2008]. In addition, age-elevation AFT data and thermal modeling of samples from Gannett Peak in the Wind River Range show a period of relatively fast cooling between ~60 Ma and ~50 Ma (equivalent to ~80°C cooling and ~4 km of exhumation assuming a geothermal gradient of 20°C/km; Figure 6). Therefore, the minimum rock uplift of the Wind River Range was 3 km, and the minimum rock uplift rate was ~0.38 mm/yr during stage 2 (~60 Ma–~52 Ma). All the major Laramide uplifts have a minimum rock uplift of 3 km during stage 2 (Table 2), because the boundary between the Precambrian basement and Phanerozoic sedimentary cover was located near sea level by the end of stage 1, and increased to at least 3 km above sea level by the end of stage 2 (Figure 7). The minimum rates of rock uplift of the other major Laramide uplifts are 0.38–0.60 mm/yr during stage 2 (Table 2).

The accelerated rock uplift during the late Paleocene–early Eocene cannot be explained by climate change. Early Cenozoic climate in Wyoming was warm and wet based on studies of vertebrate paleontology, paleobotany, paleopedology, paleosol geochemistry and carbonate clumped isotopes, and phytolith biostratigraphy [e.g., *Wilf*, 2000; *Wing et al*., 2005; *Fricke et al*., 2010; *Snell et al*., 2013; *Hyland et al*., 2013]. The wet climate condition is additionally supported by the existence of large lakes during the late Paleocene–early Eocene [e.g., *Johnson*, 1985; *Yuretich*, 1989; *Carroll et al*., 2006]. The early Cenozoic warm and wet climate culminated during the PETM (Paleocene-Eocene Thermal Maximum, ~56 Ma) and EECO (Early Eocene Climate Optimum, 53–50 Ma) [e.g., *Fricke and Wing*, 2004; *Wing et al*., 2005; *Fricke et al*., 2010; *Hyland et al*., 2013], and the high temperature may have been caused by high atmospheric pCO_2 [e.g., *Wing et al*., 2005; *Hyland et al*., 2013]. Warm and wet climate and elevated atmospheric pCO_2 intensify weathering and erosion [e.g., *Smith et al*., 2008], and the intensified erosion may cause isostatic rebound and uplift of the mountain ranges [*Stephenson and Lambeck*, 1985]. However, isostatic uplift decreases mean elevation and increases relief [*Molnar and England*, 1990], which contrast with the observed mean elevation increase and higher rock uplift rate in our data set. Therefore, isostatic uplift induced by intense erosion cannot be the driver of the accelerated rock uplift during stage 2. In addition, climate change should have caused rapid exhumation and uplift everywhere in the studied area and cannot explain how accelerated rock uplift and mean elevation gain began at different times in the Laramide mountain ranges in Wyoming.

The available data summarized above also show a southwestward trend in the timing of uplift and exhumation during the late Paleocene–early Eocene (Figure 5). The increased subsidence rate of the Powder River Basin and attainment of high elevation of its surrounding ranges in northeast Wyoming took place during late Paleocene time, slightly earlier than the other basins in central Wyoming (Figures 3, 4, and 6). The Uinta Mountains in

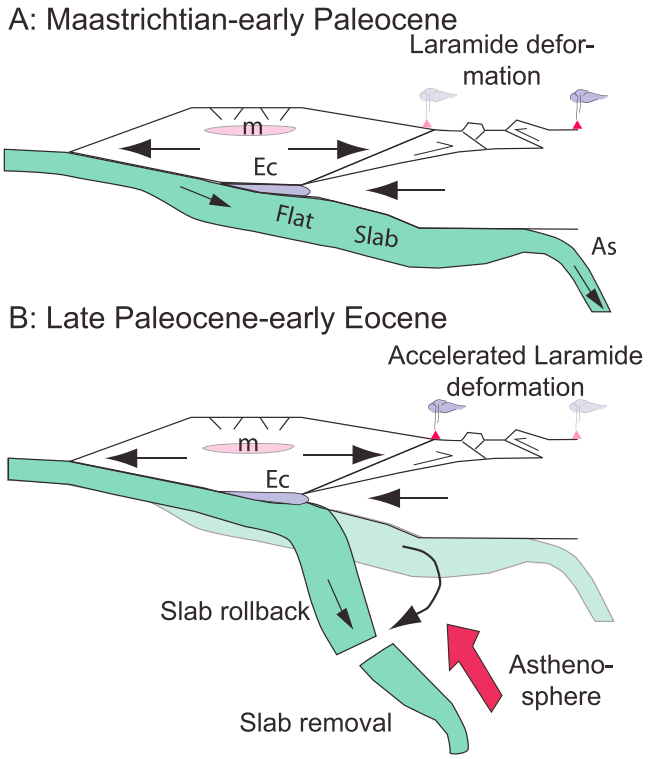

Figure 8. Schematic cross sections illustrating the principal mechanisms of the two stages of Laramide deformation. M, melt; Ec, Eclogite root; As, Asthenosphere. (a) Flat slab subduction caused northeastward deformation in the studied Rocky Mountains during the Maastrichtian–late Paleocene; the deformation may be associated with eastward migration of arc magmatism in western United States. (b) Detaching the flat slab by rolling back or removing an oceanic plateau caused hot asthenosphere upwelling and accelerated deformation during the late Paleocene–early Eocene; the deformation may be associated with westward migration of arc magmatism in Wyoming [*Constenius*, 1996]. Figures are modified after *DeCelles et al*. [2009].

southwest Wyoming attained high elevation in late early Eocene time, and the high subsidence rate in the Green River Basin continued until the middle early Eocene (Figures 3, 4, and 6). If not an artifact of imprecise geochronology, these observations suggest that accelerated deformation during stage 2 commenced earliest in northeastern Wyoming and progressed toward the southwest through time. The resulting uplift pattern is consistent with westward migration of magmatism in Wyoming [*Constenius*, 1996]. Therefore, any tectonic models explaining the accelerated deformation during stage 2 should also explain the observed southwestward trend.

5.3. Coupling Between Laramide Deformation and Different Models of Slab Subduction

Although a two-stage uplift history has been previously recognized in the Rocky Mountains and explained as a response to a change in the subduction direction of the Farallon plate, from eastward to northward, as the opening of the Norwegian Sea caused counterclockwise rotation of the North America plate [*Chapin and Cather*, 1983; *Gries*, 1983], this model cannot explain the accelerated deformation and the southwestward trend during stage 2. The history of Laramide deformation summarized above fits the prediction of geodynamic models involving flat subduction and subsequent slab removal through rollback [*Coney and Reynolds*, 1977; *Constenius*, 1996], or removal of eclogized oceanic plateau or aseismic ridges [*Liu et al*., 2008; *L. Liu et al*., 2010; *Liu and Gurnis*, 2010]. We interpret the first stage of Laramide deformation during the Maastrichtian and early Paleocene as a simple northeastward migration of strain in the greater Cordilleran orogenic system as the flat subduction proceeded (Figure 8a). This stage of deformation corresponds to when the center of the hypothetical Shatsky conjugate plateau on the Farallon plate entered southern Wyoming after it passed beneath the Colorado Plateau between 84 and 68 Ma [*L. Liu et al*., 2010; *Liu and Gurnis*, 2010; *Painter and Carrapa*, 2013]. The suction force in the asthenosphere wedge between the flat slab and Archean keel caused subsidence on the overriding plate along the southwestern edge of the Wyoming craton and produced a localized deep depocenter in southeastern Wyoming during the late Campanian and Maastrichtian [*Jones et al*., 2011; *Painter and Carrapa*, 2013]. The flattening of the slab is also consistent with the eastward magmatic sweep in Wyoming and nearby area between ~72 Ma and ~55 Ma [*Constenius*, 1996]. The physical basis for transmitting the stress from the flat slab into the crust of the overriding plate to cause crustal shortening and thickening is complex but may be approximated to a basal shear applied to the stiff Archean Wyoming craton and/or horizontal normal stress associated with end loading at the trench [e.g., *Livaccari*, 1991; *Jones et al*., 1998, 2011]. Following this logic, we suggest that the basal traction and/or horizontal normal stress caused localized uplift in the Wyoming province by reactivating preexisting structures during the Maastrichtian–late Paleocene. Because the strain was distributed across a ~400 km wide zone in Wyoming, it resulted in relatively small amounts of rock uplift for each structure.

The deformation of Sevier thrust belt may have continued until the early Eocene [e.g., *Solum and van der Pluijm*, 2007], offering an alternative explanation for the accelerated deformation during the late Paleocene–early Eocene as a simple response to strain accumulation and tectonic culmination of the Sevier deformation. However, crustal shortening and thickening in the Sevier belt cannot explain the southwestward younging trend of surface deformation in Figure 5; also, the westward magmatic sweep in Wyoming started at ~55 Ma [*Constenius*, 1996]. In addition, metamorphic core complexes and low-angle detachment faults started in the Cordilleran hinterland at ~54 Ma [e.g., *Constenius*, 1996; *Foster et al*., 2007; *Cubley et al*., 2013], suggesting a transition from shortening to extensional collapse.

Based on the observations of southwestward trend of surface elevation gain, rock uplift, and magmatic sweep, we propose that the accelerated deformation in the late Paleocene–early Eocene was associated with slab rollback, rather than continued flat-slab subduction (Figure 8b). After subduction, the flat slab steepened [e.g., *Coney and Reynolds*, 1977; *Constenius*, 1996] because of negative buoyancy of the detaching slab with respect to surrounding mantle, causing bending and trenchward retreat of the slab. Slab rollback and removal have been shown to affect uplift and exhumation on the overriding plate [e.g., *Gvirtzman and Amos*, 1999; *Wortel and Spakman*, 2000; *Buiter et al*., 2002; *Ferranti and Oldow*, 2006; *Brun and Faccenna*, 2008; *Humphrey*, 2009; *Kay and Coira*, 2009; *Göğüş et al*., 2011]. Slab rollback may have similar effects as retreating delamination of the mantle lithosphere, causing crustal deformation and magmatism on the overriding plate as a response to peeling of the mantle lithosphere away from the crust [*Krystopowicz and Currie*, 2013]. Slab rollback may be associated with lithosphere delamination of the overriding plate, causing additional surface uplift and exhumation, such as proposed for the Puna Plateau-Sierra Pampeanas [*Kay and Coira*, 2009].

Humphreys [2009] has invoked slab detachment to explain the mid-Cenozoic uplift in the Rocky Mountains, which post-dated the Laramide orogeny. Although additional evidence is required, it is possible that one segment of the Farallon oceanic plate may have steepened and subsequently detached during the late Paleocene–early Eocene, whereas the rest of the slab detached later during the mid-Cenozoic. Alternatively, *L. Liu et al*. [2010] propose that the long-term subduction of the Shatsky conjugate in the Farallon slab induced basalt-eclogite phase transformation and the loss of the oceanic slab buoyancy allowing the removal of the slab and dynamic uplift in upper crust. Regardless how the flat slab was removed, dynamic, thermal, and isostatic processes associated with slab removal may cause surface uplift and exhumation, and this uplift is not necessarily isostatically compensated [e.g., *Moucha et al*., 2008; *Liu and Gurnis*, 2010]. Such slab removal may have begun as retreating delamination of the Farallon flat slab through bending or steepening, when the rate of plate convergence was less than the rate of subduction. Although the spreading rate in the North Atlantic was high during the late Paleocene–early Eocene [*Jones et al*., 2011, Figure 4], the rate of subduction may outpace the convergent rate due to the negative buoyance of the subducting slab [e.g., *Royden*, 1993], which may be caused by the ecologitization of oceanic plateaux on the Farallon plate [*Liu et al*., 2008]. Uplift in the Wyoming province during the early Eocene was associated with the initial stage of extensional tectonics in the Sevier fold-and-thrust belt [e.g., *Constenius*, 1996; *Foster et al*., 2007; *Cubley et al*., 2013], and similar synchronous foreland uplift and hinterland extension has been documented in the southern Apennines associated with crustal delamination [*Ferranti and Oldow*, 2006].

Asthenosphere upwelling and thermal perturbation [e.g., *Moucha et al*., 2008; *Humphreys*, 2009] as well as the isostatic adjustment [e.g., *Gvirtzman and Amos*, 1999] associated with the westward peeling of the flat slab away from the overriding plate may explain the westward sweep of magmatism, extension in the Sevier hinterland, and our observed accelerated uplift and uplift/exhumation patterns during stage 2. Additional exhumation may be caused by slab detachment or delamination of mantle lithosphere of the overriding plate [*Buiter et al*., 2002; *Göğüş et al*., 2011]. Stress propagated from the mantle was added to the basal traction and/or horizontal normal stress and caused accelerated uplift of the Laramide ranges along the bounding reverse faults developed during stage 1. Dynamic, thermal, and isostatic uplift would have affected the entire Wyoming province, but local flexural subsidence associated with individual Laramide mountain ranges was evidently able to outpace the rate of dynamic uplift.

6. Summary and Conclusions

Our synthesis of paleoaltimetry, thermochronology, and provenance data and basin subsidence history in Wyoming during the Late Cretaceous–early Eocene reveal a two-stage history of Laramide deformation across

Wyoming, with significant surface elevation gain, exhumation of Laramide mountain ranges, and intermontane basin subsidence during the late Paleocene–early Eocene. By combining the magnitude of surface uplift and exhumation with regional stratigraphic cover thickness and chronostratigraphic information, we constrain the amount and rate of rock uplift of the major Laramide ranges. The amount (and rate) of rock uplift of individual Laramide ranges was less than 2.4–4.8 km (~0.21–0.32 mm/yr) during the early Maastrichtian-Paleocene and increased to more than ~3 km (~0.38–0.60 mm/yr) during the late Paleocene–early Eocene. Therefore, Laramide deformation accelerated during the late Paleocene–early Eocene. This is consistent with the observations that Laramide ranges reach high elevation ($>$ 2 km) and the basement rocks are largely exposed for erosion during this period. Our compiled results also show that surface uplift and exhumation of the major Laramide ranges appear to young southwestward during the late Paleocene–early Eocene, consistent with the timing of the westward magmatism in Wyoming.

Although the warm and wet climate and high atmosphere pCO_2 during the late Paleocene–early Eocene may have intensified erosion in the Laramide mountain ranges, isostatic rebound due to removal of topographic loads cannot explain accelerated uplift during the late Paleocene–early Eocene and the southwestward younging trend. The accelerated deformation during the late Paleocene–early Eocene also cannot be explained by tectonic culmination of the Sevier deformation because of contemporaneous extensional tectonics in the Cordillera hinterland. We propose that Laramide deformation and uplift during the early Maastrichtian-Paleocene reflects migration of the deformation front while the region was affected by flat subduction expanded northeastward, whereas the accelerated Laramide uplift and exhumation during the late Paleocene–early Eocene may be caused by the isostatic, thermal, and dynamic processes induced by removing the flat slab by slab rollback. In particular, westward slab rollback can explain the southwestward younging trend of surface uplift and exhumation as well as westward sweep of magmatism.

Acknowledgments
This work was supported by NSF grant EAR-1119005. We thank Peter DeCelles and Paul Heller for valuable discussions. Reviews by Associate Editors Nathan Niemi and Taylor Schildgen and four anonymous reviewers helped us to significantly improve the manuscript.

References

Angevine, C. L., P. L. Heller, and C. Paola (1990), *Quantitative Sedimentary Basin Modeling*, Continuing Education Course Note Series, vol. 32, 256 pp., American Association of Petroleum Geologists, Tulsa, Okla.
Beaumont, C. (1981), Foreland basins, *R.Astron. Soc. Geophys. J.*, *65*, 291–329.
Beland, P. E. (2002), Apatite fission track and (U-Th)/He thermochronology and vitrinite reflectance of the Casper Arch, Maverick Springs Dome, and the Wind River basin: Implications for Late Cenozoic deformation and cooling in the Wyoming foreland, MS thesis, Department of Geology and Geophysics, University of Wyoming, Laramie, Wyoming, U.S.A.
Berry, D. W., and R. T. Littleton (1961), Geology and ground-water resources of the Owl Creek Area, Hot Springs County, Wyoming, in *Geological Survey Water-Supply Paper*, vol. 1519, pp. 1–59, United Government Printing Office, Wash.
Bird, P. (1988), Formation of the Rocky Mountains, western United States: A continuum computer model, *Science*, *239*, 1501–1507.
Bird, P. (1998), Kinematic history of the Laramide orogeny in latitudes 35°–49°N, western United States, *Tectonics*, *17*, 780–801.
Brun, J., and C. Faccenna (2008), Exhumation of high-pressure rocks driven by slab rollback, *Earth Planet. Sci. Lett.*, *272*, 1–7.
Buiter, S. J. H., R. Grovers, and M. J. R. Wortel (2002), Two-dimensional simulations of surface deformation caused by slab detachment, *Tectonophysics*, *354*, 195–210.
Bryson, R. A., and F. K. Hare (1974), The climate of North America, in *World Survey of Climatology*, vol. 11, edited by R. A. Bryson and F. K. Hare, pp. 1–47, Elsevier, New York.
Cassel, E. J., S. A. Graham, C. P. Chamberlain, and C. D. Henry (2012), Early Cenozoic topography, morphology, and tectonics of the northern Sierra Nevada and western Basin and Range, *Geosphere*, *8*, 229–249.
Cather, S. M., C. E. Chapin, and S. A. Kelley (2012), Diachronous episodes of Cenozoic erosion in southwestern North America and their relationship to surface uplift, paleoclimate, paleodrainage, and paleoaltimetry, *Geosphere*, *8*, 1177–1206.
Carroll, A. R., L. M. Chetel, and M. E. Smith (2006), Feast to famine: Sediment supply control on Laramide basin fill, *Geology*, *34*, 197–200.
Carroll, A. R., A. C. Doebbert, A. L. Booth, C. P. Chamberlain, M. K. Rhodes-Carson, M. E. Smith, C. M. Johnson, and B. L. Beard (2008), Capture of high-altitude precipitation by a low-altitude Eocene lake, western U.S., *Geology*, *36*, 791–794.
Cerveny, P. F. (1990), Fission-track thermochronology of the Wind River Range and other basement cored uplifts in the Rocky Mountain foreland, PhD dissertation, 378 pp., University of Wyoming, Laramie, Wyoming.
Cerveny, P. F., and J. R. Steidtmann (1993), Fission track thermochronology of the Wind River range, Wyoming: Evidence for timing and magnitude of Laramide exhumation, *Tectonics*, *12*, 77–92.
Chamberlain, C. P., H. T. Mix, A. Mulch, M. T. Hren, M. L. Kent-Corson, S. J. Davis, T. W. Horton, and S. A. Graham (2012), The Cenozoic climatic and topographic evolution of the western North American Cordillera, *Am. J. Sci.*, *312*, 213–262.
Chapin, C. E., and S. M. Cather (1983), Eocene tectonics and sedimentation in the Colorado Plateau-Rocky Mountain area, in *Rocky Mountain Foreland Basins and Uplifts*, edited by J. D. Lowell and R. Gries, pp. 33–56, Rocky Mountain Association of Geologists, Denver, Colo.
Chapin, C. E., and S. M. Cather (1990), Paleogeographic and paleotectonic setting of Laramide sedimentary basins in the central Rocky Mountain region: Alternative interpretation and reply, *Geol. Soc. Am. Bull.*, *102*, 256–260.
Coney, P. J., and S. J. Reynolds (1977), Cordilleran Benioff zones, *Nature*, *270*, 403–406.
Constenius, K. N. (1996), Late Paleogene extensional collapse of the Cordilleran foreland fold and thrust belt, *Geol. Soc. Am. Bull.*, *108*, 20–39.
Coplen, T. B., and C. C. Kendall (2000), Stable hydrogen and oxygen isotope ratios for selected sites of the U.S. Geological Survey's NASQAN and Benchmark surface-water networks, *U.S. Geol. Surv. Open File Rep., 00–160*, pp. 1–409, USGS, Denver, Colo.
Courdin J. L., and J. F. Hubert (1969), Sedimentology and differentiation of sandstones in the Fort Union Formation (Paleocene), Wind River Basin, Wyoming: 21st Annual Field Conference, Wyoming Geological Association Guidebook, pp. 29–37, Casper, Wyoming.

Crews, S. G., and F. G. Ethridge (1993), Laramide tectonics and humid alluvial fan sedimentation, NE Uinta Uplift, Utah and Wyoming, *J. Sediment. Petrol.* , *63*, 420–436.
Crowley, P. D., P. W. Reiners, J. M. Reuter, and G. D. Kaye (2002), Laramide exhumation of the Bighorn Mountains, Wyoming: An apatite (U-Th)/He thermochronology study, *Geology*, *30*, 27–30.
Cross, T. A. (1989), Tectonic controls of foreland basin subsidence and Laramide style deformation, western United States, in *Foreland Basin, International Association of Sedimentologists Special Publication*, vol. 8, edited by P. A. Allen and E. Homwook, pp. 15–39, Blackwell, Oxford, U. K.
Cubley, J. F., D. R. M. Pattison, D. A. Archibald, and M. Jolivet (2013), Thermochronological constraints on the Eocene exhumation of the Grand Forks complex, British Columbia, based on $^{40}Ar/^{39}Ar$ and apatite fission track geochronology, *Can. J. Earth Sci.*, *50*, 576–598.
Dansgaard, W. (1964), Stable isotopes in precipitation, *Tellus*, *16*, 436–468.
Davis, S. J., B. A. Wiegand, A. R. Carroll, and C. P. Chamberlain (2008), the effect of drainage reorganization on paleoaltimetry studies: An example from the Paleogene Laramide foreland, *Earth Planet. Sci. Lett.*, *275*, 258–268.
Davis, S. J., H. T. Mix, B. A. Wiegand, A. R. Carroll, and C. P. Chamberlain (2009), Synorogenic evolution of large-scale drainage patterns: Isotope paleohydrology of sequential Laramide Basins, *Am. J. Sci.*, *309*, 549–602.
DeCelles, P. G., M. B. Gray, K. D. Ridgway, R. B. Cole, P. Srivastava, N. Pequera, and D. A. Pivinic (1991), Kinematic history of a foreland uplift from Paleocene synorogenic conglomerate, Beartooth Range, Wyoming and Montana, *Geol. Soc. Am. Bull.*, *103*, 1458–1475.
DeCelles, P. G., and K. N. Giles (1996), Foreland basin systems, *Basin Res.*, *8*, 105–123.
DeCelles, P. G. (2004), Late Jurassic to Eocene evolution of the Cordilleran thrust belt and foreland basin system, Western U.S.A., *Am. J. Sci.*, *304*, 105–168.
DeCelles, P. G., M. N. Ducea, P. Kapp, and G. Zandt (2009), Cyclicity in Cordilleran orogenic systems, *Nat. Geosci.*, *2*, 251–257.
Dettman, D. L., and K. C. Lohmann (2000), Oxygen isotope evidence for high-altitude snow in the Laramide Rocky Mountains of North America during the Late Cretaceous and Paleogene, *Geology*, *28*, 243–246.
Dickinson, W. R., and W. S. Snyder (1978), Plate tectonics of the Laramide orogeny, in *Laramide Folding Associated With Basement Block Faulting in the Western United States*, vol. 151, edited by V. Matthews, pp. 355–366, Geol. Soc. Am., Boulder, Colo.
Dickinson, W. R., M. A. Klute, M. J. Hayes, S. U. Janecke, E. R. Lundin, M. A. McKittrick, and M. D. Olivares (1988), Paleogeographic and paleotectonic setting of Laramide sedimentary basins in the central Rocky Mountain region, *Geol. Soc. Am. Bull.*, *100*, 1023–1039.
England, P., and P. Molnar (1990), Surface uplift, uplift of rocks, and exhumation of rocks, *Geology*, *18*, 1173–1177.
Erslev, E. A. (1993), Thrusts, back-thrusts, and detachment of Rocky Mountain foreland arches, in *Laramide Basement Deformation in the Rocky Mountain Foreland of the Western United States, Geological Society of America Special Paper*, vol. 280, edited by C. J. Schmidt, pp. 339–358, GSA, Boulder, Colo.
Fan, M., and D. L. Dettman (2009), Late Paleocene high Laramide ranges in northeast Wyoming: Oxygen isotope study of ancient river water, *Earth Planet. Sci. Lett.*, *286*, 110–121.
Fan, M., P. G. DeCelles, G. E. Gehrels, D. L. Dettman, J. Quade, and L. Peyton (2011a), Sedimentology, detrital zircon geochronology, and stable isotope geochemistry of the lower Eocene strata in the Wind River Basin, central Wyoming, *Geol. Soc. Am. Bull.*, *123*, 979–996.
Fan, M., J. Quade, D. L. Dettman, and P. G. DeCelles (2011b), Widespread basement erosion during late Paleocene-early Eocene in the Laramide Rocky Mountains inferred from $^{87}Sr/^{86}Sr$ ratios of freshwater bivalve fossils, *Geol. Soc. Am. Bull.*, *123*, 2069–2082.
Farley, K. A. (2002), (U-Th)/He dating: Techniques, calibrations, and applications, *Rev. Mineral. Geochem.*, *47*, 819–844.
Ferranti, L., and J. S. Oldow (2006), Rates of late Neogene deformation along the southwestern margin of Adria, southern Apennines orogeny, Italy, in *The Adria Microplate: GPS Geodesy, Tectonics, and Hazards*, edited by N. Pinter et al., pp. 93–116, Kluwer Academic Publisher, Dordrecht, Neth.
Fitzgerald, P. G., R. B. Sorkhabi, T. F. Redfield, and E. Stump (1995), Uplift and denudation of the central Alaska Range: A case study in the use of apatite fission-track thermochronology to determine absolute uplift parameters, *J. Geophys. Res.*, *100*, 20,175–20,191, doi:10.1029/95JB02150.
Foster, D. A., P. T. Doughty, T. J. Kalakay, C. M. Fanning, S. Coyner, W. C. Grice, and J. Vogl (2007), Kinematics and timing of exhumation of metamorphic core complexes along the Lewis and Clark fault zone, northern Rocky Mountains, USA, in *Exhumation Associated With Continental Strike-Slip Fault Systems, Geological Society of America Special Paper*, vol. 434, edited by S. M. Roeske et al., pp. 207–232, Geol. Soc. of Am., Boulder, Colo., U.S.A.
Fricke, H. C. (2003), Investigation of early Eocene water-vapor transport and paleoelevation using oxygen isotope data from geographically widespread mammal remains, *Geol. Soc. Am. Bull.*, *115*, 1088–1096.
Fricke, H. C., and S. L. Wing (2004), Oxygen isotope and paleobotanical estimates of temperature and $\delta^{18}O$-latitude gradients over North America during the early Eocene, *Am. J. Sci.*, *304*, 612–635.
Fricke, H. C., B. Z. Foreman, and J. O. Sewall (2010), Integrated climate model-oxygen isotope evidence for a North American monsoon during the Late Cretaceous, *Earth Planet. Sci. Lett.*, *289*, 11–21.
Finn, T. M., M. A. Kirschbaum, S. B. Roberts, S. M. Condon, L. N. R. Roberts, and R. C. Johnson (2010), Cretaceous-Tertiary Composite Total Petroleum System (503402), Bighorn Basin, Wyoming and Montana, in *U.S. Geol. Surv. Digital Data Series DDS–69–V*, pp. 1–157, USGS, Denver, Colo.
Flores, R. C., and F. G. Ethridge (1985), Evolution of intermontane fluvial systems of Tertiary Powder River basin, Montana and Wyoming, in *Cenozoic Paleogeography of the West Central United States: Rocky Mountain Paleogeography Symposium*, vol. 3, edited by R. M. Flores and S. S. Kaplan, pp. 107–127, Rocky Mountain Section, Society of Economic Paleontologists and Mineralogists, Denver, Colo.
Fox, J. E., and D. K. Higley (1996), Isopach maps of the Powder River Basin, Wyoming and Montana, 1:630,000, USGS Oil and Gas Investigation Chart *147-B*, USGS, Denver, Colo.
Gallagher, K., R. Brown, and C. Johnson (1998), Fission track analysis and its applications to geological problem, *Ann. Rev. Earth Planet. Sci.*, *26*, 519–572.
Göğüş, O. H., R. N. Pysklywec, F. Corbi, and C. Faccenna (2011), The surface tectonics of mantle lithosphere delamination following ocean lithosphere subduction: Insights from physical-scaled analogue experiments, *Geochem. Geophys. Geosyst.*, *12*, Q05004, doi:10.1029/2010GC003430.
Gries, B. (1983), North-south compression of Rocky Mountain Foreland structures, in *Mountain Foreland Basins and Uplifts*, edited by J. D. Lowell and R. Gries, pp. 9–32, Rocky Mountain Association of Geologists, Denver, Colo.
Gvirtzman, Z., and N. Amos (1999), Plate detachment, asthenosphere upwelling, and topography across subduction zones, *Geology*, *27*, 563–566.
Hagen, H. S., M. W. Shuster, and K. P. Furlong (1985), Tectonic loading and subsidence of intermontane basins: Wyoming foreland province, *Geology*, *13*, 585–588.
Henderson, L. J., R. G. Gordon, and D. C. Engebretson (1984), Mesozoic aseismic ridges on the Farallon plate and southward migration of shallow subduction during the Laramide orogeny, *Tectonics*, *3*, 121–132.

Hose, R. K. (1955), Geology of the Crazy Woman area, Johnson County, Wyoming, *U.S. Geol. Surv. Bull. 1027-B*, pp. 1–118, USGS, Denver, Colo.
Hough, B. G., M. Fan, and B. H. Passey (2014), Calibration of the clumped isotope geothermometer in soil carbonate in Wyoming and Nebraska, USA: Implications for paleoelevation and paleoclimate reconstruction, *Earth Planet. Sci. Lett.*, *391*, 110–120.
Hoy, R. G., and K. D. Ridgway (1997), Structural and sedimentological development of footwall growth synclines along an intraforeland uplift, east-central Bighorn Mountains, Wyoming, *Geol. Soc. Am. Bull.*, *109*, 915–935.
Humphreys, E. D. (2009), Relation of flat subduction to magmatism and deformation in the western United States, in *Backbone of the Americas: Shallow Subduction, Plateau Uplift and Ridge and Terrane Collision*, *Geol. Soc. of Am. Mem.*, vol. 204, edited by S. M. Kay, V. A. Ramos, and W. R. Dickinson, pp. 85–98, Geol. Soc. of Am., U.S.A.
Huntington, K. W., D. A. Budd, B. P. Wernicke, and J. M. Eiler (2011), Use of clumped-isotope thermometry to constrain the crystallization temperature of diagenetic calcite, *J. Sediment. Res.*, *81*, 656–669.
Hyland, E., N. D. Sheldon, and M. Fan (2013), Terrestrial paleoenvironmental reconstructions indicate transient peak warming during the early Eocene climatic optimum, *Geol. Soc. Am. Bull.*, *125*, 1338–1348.
Johnson, P. L., and D. W. Andersen (2009), Concurrent growth of uplifts with dissimilar orientations in the southern Green River Basin, Wyoming: Implications for Paleocene-Eocene patterns of foreland shortening, *Rocky Mt. Geol.*, *44*, 1–16.
Johnson, R. C. (1985), Early Cenozoic history of the Uinta and Piceance Creek basins, Utah and Colorado, with special reference to the development of Eocene Lake Uinta, in *Cenozoic Paleogeography of the West Central United States: Rocky Mountain Paleogeography Symposium*, vol. 3, edited by R. M. Flores and S. S. Kaplan, pp., 247–276, Rocky Mountain Section, Society of Economic Paleontologists and Mineralogists, Denver, Colo.
Jordan, T. E. (1981), Thrust loads and foreland basin evolution Cretaceous, western United States, *Am. Assoc. Pet. Geol. Bull.*, *65*, 2506–2520.
Jones, C. H., L. J. Sonder, and J. R. Unruh (1998), Lithospheric gravitational potential energy and past orogenesis: Implications for conditions of initial Basin and Range and Laramide deformation, *Geology*, *26*, 639–642.
Jones, G. H., L. Farmer, B. Sageman, and S. Zhong (2011), Hydrodynamic mechanism for the Laramide orogeny, *Geosphere*, *7*, 183–201.
Kay, S. M., and B. L. Coira (2009), Shallowing and steepening subduction zones, continental lithospheric loss, magmatism, and crustal flow under the central Andean Altiplano-Puna Plateau, in *Backbone of the Americas: Shallow Subduction, Plateau Uplift, and Ridge and Terrane Collision*, *Geol. Soc. of Am. Mem.*, vol. 204, edited by S. M. Kay, V. A. Ramos, and W. R. Dickinson, pp. 226–290, Geol. Soc. of Am., Boulder Colo.
Keefer, W. R. (1965), Stratigraphy and geologic history of the uppermost Cretaceous, Paleocene, and lower Eocene rocks in the Wind River Basin, Wyoming, *U.S. Geol. Surv. Prof. Pap.*, vol. 495-A, pp. 1–77, USGS, Denver, Colo.
Keefer, W. R. (1970), Structural geology of the Wind River Basin, Wyoming, *U.S. Geol. Surv. Prof. Pap.*, vol. 495-D, pp. 1–35, USGS, Denver, Colo.
Ketcham, R. A., R. A. Donelick, and W. D. Carlson (1999), Variability of apatite fission-track annealing kinetics: III. Extrapolation to geological time scales, *Am. Mineral.*, *84*, 1235–1255.
Kim, S., and J. R. O'Neil (1997), Equilibrium and nonequilibrium oxygen isotope effects in synthetic carbonates, *Geochim. Cosmochim. Acta*, *61*, 3461–3475.
Koch, P. L., J. C. Zazhos, and D. L. Dettman (1995), Stable isotope stratigraphy and paleoclimatology of the Paleogene Bighorn Basin (Wyoming, USA), *Palaeogeogr. Palaeoclimatol. Palaeoecol.*, *155*, 61–89.
Kohn, M. J., and D. L. Dettman (2007), Paleoaltimetry from stable isotope compositions of fossils, in *Paleoaltimetry: Geochemical and Thermodynamic Approaches, Reviews in Mineralogy and Geochemistry*, vol. 66, edited by M. J. Kohn, pp. 119–148, Chantilly, Virginia.
Kelley, S. A. (2005), Low-temperature cooling histories of the Cheyenne Belt and Laramie Peak shear zone, Wyoming, and the Soda Creek-Fish Creek shear zone, Colorado, in *The Rocky Mountain Region-An Evolving Lithosphere: Tectonics, Geochemistry, and Geophysics*, *American Geophysical Union Monograph*, vol. 154, edited by K. E. Karlstrom and G. R. Keller, pp. 55–70, AGU, Washington, D. C.
Krystopowics, N. J., and C. A. Currie (2013), Crustal eclogitization and lithosphere delamination in orogens, *Earth Planet. Sci. Lett.*, *361*, 195–207.
Lechler, A. R., and N. A. Niemi (2011a), isotope-based paleoaltimetry and hydrologic studies surface waters in the southwestern United States: Implications for stable isotope-based paleoaltimetry and hydrologic studies, *Geol. Soc. Am. Bull.*, *124*, 318–334.
Lechler, A. R., and N. A. Niemi (2011b), Controls on the spatial variability of modern meteoric $\delta^{18}O$: Empirical constraints from the western U.S. and east Asia and implications for stable isotope studies, *Am. J. Sci.*, *311*, 664–700.
Lee, J., and I. Fung (2008), "Amount effect" of water isotopes and quantitative analysis of post-condensation processes, *Hydrol. Processes*, *22*, 1–8.
LeFebre, G. B. (1988), Tectonic evolution of Hanna Basin, Wyoming: Laramide block rotation in the Rocky Mountain foreland, PhD dissertation, 480 pp., University of Wyoming, Laramie, Wyoming.
Liu, L., S. Spasojevi, and M. Gurnis (2008), Reconstructing Farallon plate subduction beneath North America back to the late Cretaceous, *Science*, *322*, 934–938.
Liu, L., and M. Gurnis (2010), Dynamic subsidence and uplift of the Colorado Plateau, *Geology*, *38*, 663–666.
Liu, L., M. Gurnis, M. Seton, J. Saleeby, R. D. Muller, and J. Jackson (2010), The role of oceanic plateau subduction in the Laramide orogeny, *Nat. Geosci.*, *3*, 353–357.
Liu, Z., G. J. Bowen, and J. M. Welker (2010), Atmospheric circulation is reflected in precipitation isotope gradients over the conterminous United States, *J. Geophys. Res.*, *115*, D22120, doi:10.1029/2010JD014175.
Livaccari, R. F., K. Burke, and A. M. C. Sengor (1981), Was the Laramide orogeny related to subduction of an oceanic plateau?, *Nature*, *289*, 276–278.
Livaccari, R. F. (1991), Role of crustal thickening and extensional collapse in the tectonic evolution of the Sevier-Laramide orogeny, western United States, *Geology*, *19*, 1104–1107.
McQuarrie, N., and C. G. Chase (2000), Raising the Colorado Plateau, *Geology*, *28*, 91–94.
McMillan, M. E., P. L. Heller, and S. L. Wing (2006), History and causes of post-Laramide relief in the Rocky Mountain orogenic plateau, *Geol. Soc. Am. Bull.*, *118*, 393–405.
Merewether, E. A., and W. A. Cobban (1986), Biostratigraphic units and tectonism in the mid-Cretaceous foreland of Wyoming, Colorado, and adjoining area, in *Paleotectonics and Sedimentation in the Rocky Mountain Region, United States*, American Association of Petroleum Geologist Memoir, vol. 41, edited by J. A. Peterson, pp. 443–468, American Association of Petroleum Geologist, U.S.A.
Morrill, C., and P. L. Koch (2002), Elevation or alteration? Evaluation of isotopic constraints on paleoaltitudes surrounding the Eocene Green River Basin, *Geology*, *30*, 151–154.
Molnar, P., and P. England (1990), Late Cenozoic uplift of mountain ranges and global climate change: Chicken or egg?, *Nature*, *345*, 29–34.
Moucha, R., A. M. Forte, D. B. Rowley, J. X. Mitrovia, N. A. Simmons, and S. P. Grand (2008), Mantle convection and the recent evolution of the Colorado Plateau and the Rio Grande Rift valley, *Geology*, *36*, 439–442.

Norris, R. D., L. S. Jones, R. M. Corfield, and J. E. Cartlidge (1996), Skiing in the Eocene Uinta Mountains? Isotopic evidence in the Green River Formation for snow melt and large mountains, *Geology*, *24*, 403–406.
Omar, G. I., T. M. Lutz, and R. Giegengack (1994), Apatite fission-track evidence for Laramide and post-Laramide uplift and anomalous thermal regime at the Beartooth overthrust, Montana-Wyoming, *Geol. Soc. Am. Bull.*, *106*, 74–85.
Parker, S. E., and R. W. Jones (1986), Isopachous map of the Tertiary overburden above the latest Cretaceous Lance Formation, Bighorn Basin, Wyoming, 1:250,000, Wyoming State, *Geol. Surv. Open File Rep. 86–8*, Laramie, Wyoming.
Painter, C., and B. Carrapa (2013), Flexural versus dynamic processes of subsidence in the North America Cordillera foreland basin, *Geophys. Res. Lett.*, *40*, 4249–4253, doi:10.1002/grl.50831.
Passey, B. H., N. E. Levin, T. E. Cerling, F. H. Brown, and J. M. Eiler (2010), High-temperature environments of human evolution in East Africa based on bond ordering in paleosol carbonates, *Proc. Natl. Acad. Sci. U.S.A.*, *107*, 11,245–11,249.
Peyton, S. L., P. W. Reiners, B. Carrapa, and P. G. DeCelles (2012), Low-temperature thermochronology of the northern Rocky Mountains, western U.S.A., *Am. J. Sci.*, *321*, 145–212.
Peyton, S. L., and B. Carrapa (2013), An overview of low-temperature thermochronology in the Rocky Mountains and its application to petroleum system analysis, in *Application of Structure Methods to Rocky Mountain Hydrocarbon Exploration and Development*, vol. 65, edited by C. Knight, J. Cuzella, and L. D. Cress, pp. 37–70, AAPG and RMAG, Tulsa, Okla.
Pollastro, R. M., and C. E. Barker (1984), Geothermometry from clay minerals, vitrinite reflectance, and fluid inclusions—Applications to the thermal and burial history of rocks cored from the Wagon Wheel No.1 Well, Green River Basin, Wyoming, in *Geological Characteristics of Low-Permeability Upper Cretaceous and Lower Tertiary Rocks in the Pinedale Anticline Area, Sublette County, Wyoming*, edited by B. E. Law, *U.S. Geol. Surv. Open File Rep. 84–753*, pp. 78–94, USGS, Denver, Colo.
Quade, J., C. Garzione, and J. Eiler (2007), Paleoelevation reconstruction using pedogenic carbonates, in *Paleoaltimetry: Geochemical and Thermodynamic Approaches, Reviews in Mineralogy and Geochemistry*, vol. 66, edited by M. J. Kohn, pp. 53–87, Chantilly, Virginia.
Roberts, L. N. R., and M. A. Kirschbaum (1995), Paleogeography of the Late Cretaceous of the Western Interior of middle North America: Coal distribution and sediment accumulation, in *U.S. Geol. Surv. Prof. Pap. 16–1561*, pp. 1–155, USGS, Denver, Colo.
Royden, L. H. (1993), Evolution of retreating subduction boundaries formed during continental collision, *Tectonics*, *12*, 629–638.
Rowley, D. B. (2007), Stable isotope-based paleoaltimetry: Theory and validation, in *Paleoaltimetry: Geochemical and Thermodynamic Approaches, Reviews in Mineralogy and Geochemistry*, vol. 66, edited by M. J. Kohn, pp. 23–52, Chantilly, Virginia.
Royse, F., Jr., M. A. Warner, and D. L. Reese (1975), Thrust belt structural geometry and related stratigraphie problems, Wyoming-Idaho-northern Utah, in *Symposium on Deep Drilling Frontiers of the Central Rocky Mountains*, edited by D. W. Bolyard, pp. 41–54, Rocky Mountain Association of Geologists, Denver, Colorado.
Retallack, G. J. (2005), Pedogenic carbonate proxies for amount and seasonality of precipitation in paleosols, *Geology*, *33*, 333–336.
Saleeby, J. (2003), Segmentation of the Laramide Slab—Evidence from the southern Sierra Nevada region, *Geol. Soc. Am. Bull.*, *115*, 665–668.
Schwartz, R. K., and P. G. DeCelles (1988), Foreland basin evolution and synorogenic sedimentation in response to interactive Cretaceous thrusting and reactivated foreland partitioning, in *Interaction of the Rocky Mountain Foreland and the Cordilleran Thrust Belt*, *Geol. Soc. of Am. Mem.*, vol. 171, edited by C. J. Schmidt and W. J. Perry Jr., pp. 489–513, Geol. Soc. of Am., U.S.A.
Smith, M. E., A. R. Carroll, and E. R. Mueller (2008), Elevated weathering rates in the Rocky Mountains during the Early Eocene Climatic Optimum, *Nat. Geosci.*, *1*, 370–374.
Snell, K. E., B. L. Thrasher, J. M. Eiler, P. L. Koch, L. C. Sloan, and N. J. Tabor (2013), Hot summers in the Bighorn Basin during the early Paleogene, *Geology*, *41*, 55–58.
Snell, K. E., P. L. Koch, P. Druschke, B. Z. Foreman, and J. M. Eiler (2014), High elevation of the 'Nevadaplano' during the Late Cretaceous, *Earth Planet. Sci. Lett.*, *386*, 52–63.
Snyder, W. S., W. R. Dickinson, and M. L. Silberman (1976), Tectonic implications of space-time patterns of Cenozoic magmatism in the Western United States, *Earth Planet. Sci. Lett.*, *32*, 91–106.
Solum, J. G., and B. A. van der Pluijm (2007), Reconstructing the Snake River-Hoback River Canyon section of the Wyoming thrust belt through direct dating of clay-rich fault rocks, in *Whence the Mountains? Inquiries Into the Evolution of Orogenic Systems: A Volume in Honor of Raymond A. Price*, *Geological Society of America Special Paper*, vol. 433, edited by J. W. Sears, T. A. Harms, and C. A. Evenchick, pp. 183–196, Geol. Soc. of Am., U.S.A.
Sprinkel, D. A. (2000), Geologic guide along Flaming Gorge Reservoir, Flaming Gorge National Recreation Area, Utah-Wyoming, in *Geologic Road, Trail, and Lake Guides to Utah's Parks and Monuments*, vol. 29, edited by P. B. Anderson and D. A. Sprinkel, pp. 1–20, Utah Geological Association Publication, Utah Geological Survey, Salt Lake City, Utah.
Steckler, M. S., and A. B. Watts (1978), Subsidence of the Atlantic type continental margin off New York, *Earth Planet. Sci. Lett.*, *41*, 1–13.
Steidtmann, J. R., and L. T. Middleton (1991), Fault chronology and uplift history of the southern Wind River Range, Wyoming: Implications for Laramide and post-Laramide deformation in the Rocky Mountains foreland, *Geol. Soc. Am. Bull.*, *103*, 472–485.
Stephenson, R., and K. Lambeck (1985), Erosion-isostatic rebound models for uplift: An application to south-eastern Australia, *Geophys. J. R. Astron. Soc.*, *82*, 31–55.
Strecker, U. (1996), Studies of Cenozoic continental tectonics, PhD dissertation, 686 pp., University of Wyoming, Laramie, Wyoming.
Sewall, J. O., and L. C. Sloan (2006), Come a little bit closer: A high-resolution climate study of the early Paleogene Laramide foreland, *Geology*, *34*, 81–84.
Tarduno, J. A., M. McWilliams, M. G. Debiche, W. V. Sliter, and M.C.Jr, Blake (1985), Franciscan Complex Calera limestones: Accreted remnants of Farallon Plate oceanic plateaus, *Nature*, *317*, 345–347.
Vachon, R., J. Welker, J. White, and B. Vaughn (2010), Monthly precipitation isoscapes ($\delta^{18}O$) of the United States: Connections with surface temperatures, moisture source conditions, and air mass trajectories, *J. Geophys. Res.*, *115*, D21126, doi:10.1029/2010JD014105.
White, P. (2005), The stable isotope stratigraphy and paleosols of North America's most southern exposure of late Paleocene/Early Eocene fossiliferous continental deposits documenting the initial Eocene thermal maximum in Big Bend National Park, Texas, PhD dissertation, 108 pp., Louisiana State University, Baton Rough, Louisiana.
Whipkey, C. E., V. V. Cavaroc, and R. M. Flores (1991), Uplift of the Bighorn Mountains, Wyoming and Montana—A Sandstone provenance study, *U.S. Geol. Surv. Bull. 1917-D*, pp. 1–28, USGS, Denver, Colo.
Winterfeld, G. F., and J. B. Conard (1983), Laramide tectonics and deposition, Washakie Range and northwestern Wind River Basin, Wyoming, in *Rocky Mountain Foreland Basins and Uplifts*, edited by J. D. Lowell and R. Gries, pp. 137–148, Rocky Mountain Association of Geologists, Denver, Colo.
Wilf, P. (2000), Late Paleocene–early Eocene climate changes in southwestern Wyoming: Paleobotanical analysis, *Geol. Soc. Am. Bull.*, *112*, 292–307.
Wing, S. L., G. J. Harrington, F. A. Smith, I. B. Jonathan, D. M. Boyer, and K. H. Freeman (2005), Transient floral change and rapid global warming at the Paleocene-Eocene boundary, *Science*, *310*, 993–996.

Wise, D. U. (1957), Tectonics and tectonic heredity in the southern Beartooth Mountains, Wyoming, PhD dissertation, 374 pp., Princeton University, Princeton, N. J.
Wolfe, J. A., C. E. Forest, and P. Molnar (1998), Paleobotanical evidence of Eocene and Oligocene paleoaltitudes in midlatitude western North America, *Geol. Soc. Am. Bull.*, *110*, 664–678.
Wortel, M. J. R., and W. Spakman (2000), Subduction and slab detachment in the Mediterranean-Carpathia region, *Science*, *290*, 1910–1917.
Yuretich, R. (1989), Paleocene lakes of the central Rocky Mountains, western United States, *Palaeogeogr. Palaeoclimatol. Palaeoecol.*, *70*, 53–63.
Zachos, J. C., L. D. Stott, and K. C. Lohmann (1994), Evolution of marine temperatures during the Palaeogene, *Paleoceanography*, *9*, 353–387.
Zachos, J. C., M. Pagani, L. Sloan, E. Thomas, and K. Billup (2001), Trends, rhythms, and aberrations in global climate 65 Ma to present, *Science*, *292*, 686–693.